Network Reconstruction Problem for an Epidemic Reaction-Diffusion System

Louis-Brahim Beaufort[§], Pierre-Yves Massé[§], Antonin Reboulet and Laurent Oudre
Université Paris-Saclay, ENS Paris-Saclay, CNRS,
Centre Borelli, F-91190, Gif-sur-Yvette, France

May 2022

Abstract

We study the network reconstruction problem for an epidemic reaction-diffusion system. These systems are an extension of deterministic, compartmental models to a graph setting, where the reactions within the nodes are coupled by a diffusion dynamics. We study the influence of the diffusion rate, and the network topology, on the reconstruction and prediction problems, both from a theoretical and experimental standpoint. Results first show that for almost every network, the reconstruction problem is well-posed. Then, we show that the faster the diffusion dynamics, the harder the reconstruction, but that increasing the sampling rate may help in this respect. Second, we demonstrate that it is possible to classify symmetrical networks generating the same trajectories, and that the prediction problem can still be solved satisfyingly, even when the network topology makes exact reconstruction difficult.

Keywords. Epidemic models, network reconstruction, reaction-diffusion, graph automorphisms

Contents

1 Introduction **3**

2 Background and related work **4**
2.1 Deterministic, Compartmental Epidemiological Models 4
2.2 Background on Issues in Network Reconstruction 5
2.3 Background on Network Topology and Symmetries 7
2.4 Contributions of the article 7

3 Model, Definitions and Notations **8**
3.1 Reaction-Diffusion Systems 8

[§]Equal contribution

3.2 Network Reconstruction 10
3.3 Symmetries 11

4 Well-Posedness, Diffusion Rate and Symmetries **12**
4.1 Well-Posedness of the Reconstruction Problem 12
4.2 Diffusion Rate 13
4.3 Symmetries 14

5 Numerical Simulations **15**
5.1 Numerical Simulations Set-Up 16
5.2 Influence of the Diffusion Rate 18
5.3 Influence of the Network Topology 19
5.4 Influence of Noise 21
5.5 Semi-Real Data Example 22

6 Conclusions, future works **24**

7 Proofs for Section 4.1, Well-Posedness of the Reconstruction Problem **26**

8 Proofs for Section 4.2, analysis of the influence of the diffusion rate **29**

9 Proofs for Section 4.3, symmetries **32**

References **35**

1 Introduction

Network reconstruction problems, in which one aims at reconstructing a network structure from the observation of a signal evolving on it, is an important topic of current research, spanning over numerous domains (Timme and Casadiego 2014; Shandilya and Timme 2011; Dong et al. 2015; Le Bars et al. 2019; Sardellitti, Barbarossa, and Lorenzo 2019; Asllani et al. 2020; Emary and Fort 2021). Indeed, the widespread use of networks as a modelling tool in fields as diverse as telecommunications (Pastor-Satorras and Vespignani 2004; M. E. J. Newman, Watts, and Strogatz 2002), genetics (Gardner et al. 2003; Karlebach and Shamir 2008), ecology (Hanski and Gilpin 1997; Tamburello, O. Ma, and M. Côté 2019), or transportation of goods or humans (Youn, Gastner, and Jeong 2008; Perfido et al. 2017), to name but a few, makes understanding the connections between their structure, or internal properties, and the phenomena which happen over them, a crucial issue.

A popular framework to study propagation phenomena on networks are deterministic epidemic models (Nowzari, Victor M. Preciado, and Pappas 2016). These models have gained considerable attention since the early 20th century, following notably the classic works of Kermack and McKendrick (1927). In those, individuals are categorized in compartments which describe their status with respect to an infectious disease, and the models describe the way they transition from compartments to compartments as the disease spreads through contacts, and they react (heal) to it (Diekmann, H. Heesterbeek, and Britton 2012). Quickly, the early scalar models have been enhanced, by embedding them into networks (Pastor-Satorras and Vespignani 2001; Pastor-Satorra et al. 2015; Nowzari, Victor M. Preciado, and Pappas 2016), in order to refine the analysis of the influence of contacts between individuals, on the spread of the disease.

Recently, Prasse and Van Mieghem (2020a) have addressed the reconstruction problem for a wide class of epidemic models (Nowzari, Victor M. Preciado, and Pappas 2016). In their work, they ask two questions: first, can the network structure be retrieved from the observation of the dynamics? Secondly, even in the case of a negative answer, is it possible to approximate the structure well enough to predict the future evolution of the disease? Even if the problem they study has a linear structure, they show the answers to these questions are not straightforward. We propose to address the same questions on another very important class of network-epidemic models, the epidemic reaction-diffusion models, also known as metapopulation models with explicit movement (Arino 2009). Just like the model studied in Prasse and Van Mieghem (2020a), the nodes of the graph represent subpopulations: for instance, the cities in the transportation network of a country. However, the interactions between populations is no longer described by a static contact structure, but by a diffusion dynamics. Accordingly, the internal dynamics of each sub-population follows a standard deterministic epidemic model (SIS, SEIR, ...) (Diekmann, H. Heesterbeek, and Britton 2012) while flows of individuals go from node to node through a diffusion dynamics. Following their apparition in population dynamics in the 1970's, these models have since gained considerable attention in the field of mathematical epidemiology (Brauer and Driessche 2001;

Van den Driessche and Watmough 2002; W. Wang and Zhao 2005; Allen et al. 2007; Tien et al. 2015; Arino 2017; Soriano-Paños et al. 2022). However, we are not aware the inverse problem has been studied for these models, up to now.

We therefore propose to conduct a case-study in network reconstruction for epidemic reaction-diffusion models. On the one hand, it contributes in exploring a new (up to our best knowledge) line of work on these models, and also furthers the general works on network reconstruction for network epidemic models. On the other hand, it contributes to network reconstruction studies by showing their usefulness on yet another setting. First, we conduct a theoretical analysis of the system, studying the role played by the speed of diffusion, and the symmetries of the network, in making reconstruction more difficult. Second, we illustrate numerically our findings related to the speed of diffusion, and study the reconstruction, and prediction, problems for different network topologies, before considering the impact of noise on the reconstruction.

We first present background material and related works in Section 2. Next, we define the model we study, and introduce our notations, in Section 3. Then, we study reconstruction from a theoretical standpoint in Section 4. Finally, we conduct numerical simulations in Section 5. The proofs are deferred to the appendices. The code for the simulations, implemented in Python, is available on the git repository: https://reine.cmla.ens-cachan.fr/masse/network_reconstruction_reaction_diffusion.

2 Background and related work

We first present the classical epidemiological models (Section 2.1), before giving a short overview on network reconstruction techniques (Section 2.2), and symmetries (2.3). Finally, we present our contributions (Section 2.4).

2.1 Deterministic, Compartmental Epidemiological Models

Deterministic, compartmental epidemiological models represent the propagation of a disease within a population by first segmenting the population in compartments, describing the status with respect to the disease (Diekmann, H. Heesterbeek, and Britton 2012). Classical compartments include the "susceptible" (S), which gathers people which may contract the disease when confronted to "infected" (I) people, who later will have "recovered" (R). Transitions from compartments to compartments are governed by differential equations. One simple and generic model, which we use for simplicity throughout our study, is the SIR model. Three scalar functions s, i and r track the numbers of people in each compartment, and they evolve according

to, for all $t \geq 0$,

$$\begin{cases} \dfrac{ds}{dt} = -\beta si \\ \dfrac{di}{dt} = \beta si - \delta i \\ \dfrac{dr}{dt} = \delta i. \end{cases} \tag{1}$$

The parameter β is often called the infection rate, and δ is the curing rate. The quantity δ^{-1} may be interpreted as the average time an individual remains infected, before healing (Diekmann, J. A. P. Heesterbeek, and Roberts 2009). The fact δ is positive means people heal in finite time. It is well-known that the system of Equation (1) has a global solution for every initial condition (s_0, i_0, r_0) with only nonnegative coordinates, and that solutions tend to equilibria of the form $(s_\infty, 0, r_\infty)$ (Diekmann, H. Heesterbeek, and Britton 2012).

Works have extended these models to graphs, in order to increase their representative power (Nowzari, Victor M. Preciado, and Pappas 2016). Nodes of the graphs represent either individuals, or sub-populations (cities, or countries, for instance). The coupling between the nodes may be static (Nowzari, Victor M. Preciado, and Pappas 2016): individuals remain in their node, and can be infected by individuals in nodes with which their node has contacts. In our work, we consider a diffusive coupling (Brauer and Driessche 2001; Van den Driessche and Watmough 2002; W. Wang and Zhao 2005; Allen et al. 2007; Tien et al. 2015; Arino 2017), whereby individuals can only be infected by other individuals in the same node, but move through the graph according to a diffusion dynamics.

2.2 Background on Issues in Network Reconstruction

The network reconstruction problem from observations, where one aims at explicitiing the topology of a network of N nodes, by observing the values taken by some dynamical system which evolves on it, has been extensively studied in the literature (see for instance the review Timme and Casadiego (2014)). Angulo et al. (2017) characterize the theoretically necessary conditions on the structure of the dynamic system of the network, and on the measured data, for the reconstruction to be possible. Asllani et al. (2020) focus on the role of the interplay between node level versus network level dynamics. The network is described by some matrix, typically, the adjacency matrix, possibly weighted. Observations are often gathered in two matrices. The first matrix gathers estimates of the time derivatives of the state of the dynamical system in each node, at the different measurement times. The second matrix is the so-called observation matrix, and gathers the values in each node, at the same times. Then, the three matrices satisfy a linear relation, and the reconstruction problem may be solved by regression. We first describe the different observations possible, then address the issue of solving the regression.

Observations may first consist in measurements of the answer the system gives to some user-driven perturbation of its dynamics (Gardner et al. 2003; Yeung, Tegnér, and Collins 2002; Yu and Parlitz 2010). In the case of non linear dynamics, these

perturbations may occur near a fixed point, the interest being that the first-order expansion of this system then depends linearly on the network (Gardner et al. 2003). Alternatively, observations may be obtained through mere observation of the system (Shandilya and Timme 2011; Makarov, Panetsos, and Feo 2005; Young, Cantwell, and M E J Newman 2021). The nature of the exact regression problem to solve moreover depends on whether a model for the dynamics studied is known (Shandilya and Timme 2011; Gardner et al. 2003; W.-X. Wang et al. 2011; Prasse and Van Mieghem 2020a), or not (Quinn et al. 2011; Barzel and Barabàsi 2013; Mangan et al. 2016; Casadiego et al. 2017). For instance, in Bussel, Kriener, and Timme (2011), the authors use detailed knowledge of the evolution of a synthetic model of a biological synaptic network between spiking times, to obtain the relation satisfied by the network matrix. On the other hand, (Casadiego et al. 2017) only assume some very general relation between the first order derivatives of the dynamical system, and the values it takes, in order to obtain similar relations. Li et al. (2017) propose a principled data-based method to linearize the switching probabilities of binary state dynamics, for a broad range of monotonic switching functions.

Once obtained the observations characterising the network matrix, one must then solve the regression problem. It may be over, or under determined, (Stoer and Burlisch 1993). Even when it is well determined, it may be ill-conditioned, thus preventing efficient solving by mere matrix inversion. To address these issues, a standard choice is to minimise the regression error with respect to some norm. One choice is then between L^1 or L^2 (least-squares) optimisation. The former induces sparsity, which may be desirable. For instance, Mangan et al. (2016) assume the dynamics decompose in some well-chosen basis, and that most of the coefficients in the expansion vanish. They then identify a subspace to which the vector of coefficients belongs, and finally use standard algorithms to find the sparsest vector in this subspace. Z. Shen et al. (2014) use compressed sensing to recover the network structure, and the infection and curing rates, in a stochastic setting. In Yeung, Tegnér, and Collins (2002), the authors use an SVD decomposition of some observation matrix to parametrize the set of networks consistent with the data, and then use sparse regression to find the sparsest such network. In W.-X. Wang et al. (2011), the authors decompose the dynamics over some infinite basis, then use compressed sensing to evaluate the coefficients, only few of them are then nonzero. In Ma, Han, et al. (2015), the authors reconstruct undirected, heterogeneous networks by notably identifying nodes where link-reconstruction suggestions are contradictory, and overriding them with more consistent information providing nodes. Least-square optimization is on the other hand less costly, and better suited for over-determined systems. In Prasse and Van Mieghem (2020a), the authors use a least-square optimisation, but add a L^1 penalty in order to enforce some degree of sparsity.

Let us also briefly mention the following works. Tyrcha and Hertz (2014), in another vein, differentiate the dynamics of the model, in order to train it to reproduce the observations, as is usual for Recurrent Neural Networks. Ma, Liu, and Van Mieghem (2019) study the correlation between the epidemic prevalence in deterministic, static-contact network epidemic dynamics and various metrics of the network, in order to determine those which can be recovered from this precise in-

formation. Surano et al. (2019) use a statistical procedure to recover the backbone of a temporal network. Finally, Peixoto (2019) proposed a Bayesian framework for network reconstruction in the presence of stochastic dynamics, where the posterior distribution of the observed data is optimised through a Metropolis-Hastings algorithm, and Braunstein, Ingrosso, and Muntoni (2019) used belief propagation also in a Bayesian setting.

2.3 Background on Network Topology and Symmetries

The topology of the network plays an important role in the behaviour of the system evolving on it. For instance, Ganesh, Massoulié, and Towsley (2005) and Durrett (2010) relate the behaviour of a stochastic epidemic dynamics to the (possibly asymptotic) properties of random graphs. Vajdi and Scoglio (2018) focus on recovering missing links in the presence of some degree of information about the underlying structure.

One peculiar kind of topological feature is the presence of symmetries in the graph. Also known as automorphisms of a graph, they are known to be a useful tool to analyse the behaviour of coupled systems of differential equations, whose coupling is described by this graph (Golubitsky and Stewart 2006). They contribute to explain qualitative behaviours, such as synchronization, of physical systems (Pecora et al. 2014; Salova and D'Souza 2020). In Broom and Rychtář (2008), the authors relate the group of automorphisms of the graph to the patterns formed by the Markov chain evolving on the graph they study. Computing the automorphisms group of a graph may also help find a lumping of a differential, or stochastic, system evolving on the graph. A lumping is a lower-dimensional system which contains all information about the bigger it was computed from (Filliger and Hongler 2008). This was notably used for epidemiological models Simon, Taylor, and Kiss (2011), Ward and López-García (2019), and Prasse, Devriendt, and Van Mieghem (2021). Symmetries have been shown to occur in many real world networks (MacArthur, Sánchez-García, and Anderson 2008), which further highlights their relevance for the study of models unfolding on networks. Finally, Rosell-Tarragó and Díaz-Guilera (2021) study a weakened notion of "quasi-symmetries" on networks.

2.4 Contributions of the article

In our work, we study the reconstruction, and prediction, problems, for an epidemic reaction-diffusion system. We assume known an epidemic model, and we consider that observations are a given, standalone time-series. Theoretically, we show that

- for almost every network, the reconstruction problem is well-posed (Proposition 7);
- the quicker the diffusion dynamics, the lower the numerical rank of the observation matrix (Corollary 9);
- the presence of symmetries in the trajectories is equivalent to the existence of symmetrical networks generating them (Proposition 10).

Notation	Definition	Meaning
N	integer	size of the graph
$u \odot v$	$(u_n v_n)_{1 \leq n \leq N} \in \mathbb{R}^N$	coordinate-wise product
1_N	$(1, \ldots, 1) \in \mathbb{R}^N$	unit vector
$\mathbb{R}V$	$V \in \mathbb{R}^N$	line directed by the vector V
$\mathcal{E}_1 \oplus \mathcal{E}_2$	$\mathcal{E}_1$, $\mathcal{E}_2$ vector spaces	direct sum
$\mathfrak{S}_N$	—	symmetric group of order N
$\mathcal{N}$	—	nodes set of the graph
$\mathcal{E}$	—	edges set of the graph
n	integer, $1 \leq n \leq N$	node of the graph
β_n	$\beta_n > 0$	infection rate of node n
δ_n	$\delta_n > 0$	curing rate of node n
$\boldsymbol{\beta}$	$(\beta_1, \ldots \beta_N) \in \mathbb{R}^N$	vector
$\boldsymbol{\delta}$	$(\delta_1, \ldots \delta_N) \in \mathbb{R}^N$	vector
s, i, r	$s, i, r \in \mathbb{R}_+$, or such-valued time trajectories (e.g. $t \mapsto s(t)$)	compartments or trajectories, scalar systems
S, I, R	$S, I, R \in \mathbb{R}_+^N$, or such-valued time trajectories (e.g. $t \mapsto S(t)$)	compartments or trajectories, graph systems
X	$X = (S, I, R) \in \mathbb{R}_+^{3N}$, with $S, I, R \in \mathbb{R}_+^N$, or trajectory	state of system, or trajectory
$\Phi_t(\mathcal{C})$	$\Phi_t(\mathcal{C}) = (S(t), I(t), R(t)) \in \mathbb{R}_+^{3N}$	Value at t of the flow associated to the configuration $\mathcal{C}$ (Definition 4).
$\mathbf{C}\left(\mathbb{R}_+, \mathbb{R}^{3N}\right)$	—	Space of continuous functions from $\mathbb{R}_+$ to $\mathbb{R}^{3N}$

Table 1: Notations

Technique-wise, our works leverages known tools in network reconstruction, addressing the same questions as Prasse and Van Mieghem (2020a): we try to reconstruct the network, and to predict the future evolution of the dynamics. Unlike them, we study a reaction-diffusion dynamics (Arino 2009) instead of a system with static coupling. Contrary to works using symmetries as an help to reduce the size of the system they study (Ward and López-García 2019), we show that they have an adverse effect in our case, as they reduce the rank of the observation matrix, and therefore lead to not well-posed reconstruction problems.

3 Model, Definitions and Notations

We define the model we study, and we make notations we use precise. We first introduce the reaction-diffusion system we study (Section 3.1), then we give notations concerning network reconstruction (Section 3.2), and we conclude with symmetries (Section 3.3). All main notations are gathered in Table 1.

3.1 Reaction-Diffusion Systems

We write $(\mathcal{N}, \mathcal{E})$ a possibly directed, (strongly, if directed) connected graph of N nodes, where $\mathcal{N}$ is the nodes set, and $\mathcal{E}$ is the edges set. The positive vectors $\boldsymbol{\beta} = (\beta_1, \ldots, \beta_N)$ and $\boldsymbol{\delta} = (\delta_1, \ldots, \delta_N)$ gather the epidemiological parameters associated to each node of the graph (details about their meaning are given in Section 2.1).

Diffusion dynamics on the graph are governed by a diffusion matrix[1], which is defined as follows.

Definition 1 (Diffusion Matrix)**.** *A diffusion matrix* M *on* $(\mathcal{N}, \mathcal{E})$ *first has nonzero entries only for nodes* i, j *such that there is an edge* $i \rightsquigarrow j$ *in* $\mathcal{E}$*. Secondly, the matrix* M *is Metzler, that is for* $i \neq j$*, we have* $\mathrm{M}_{ij} \geq 0$*. Thirdly, it is irreducible*[2]*. Finally, the sum of the coefficients of every column is* 0*.*

Standard Perron-Frobenius theory (Meyer 2000) shows a diffusion matrix admits a unique stationary distribution, that is a positive vector $\tilde{\mu}_{\mathrm{M}}$ summing to 1 such that $\mathrm{M}\tilde{\mu}_{\mathrm{M}} = 0$. Moreover, it shows that the space decomposes as the direct sum $\mathbb{R}^N = \mathbb{R}\tilde{\mu}_{\mathrm{M}} \oplus \mathcal{H}$, where $\mathbb{R}\tilde{\mu}_{\mathrm{M}}$ is the line directed by $\tilde{\mu}_{\mathrm{M}}$, and $\mathcal{H} = \left\{\nu \in \mathbb{R}^N \,|\, \sum_n \nu_n = 0\right\}$ is the image of M. In particular, this implies that, in this decomposition, the projection of any vector $V \in \mathbb{R}^N$ onto $\tilde{\mu}_{\mathrm{M}}$ is $\left(\sum_n V_n\right)\tilde{\mu}_{\mathrm{M}}$. In parts of our work, we renormalise the diffusion matrix by a real number $\tau > 0$, which we call the typical time of diffusion. Conversely, $1/\tau$ is the rate of diffusion. Finally, we sometimes use M^* to denote the "true" diffusion matrix, which we aim at reconstructing.

Definition 2 (Reaction-Diffusion System)**.** *The reaction-diffusion dynamics we study is given by*

$$\begin{cases} \dfrac{dS}{dt} = -\boldsymbol{\beta} \odot S \odot I + \mathrm{M}S \\ \dfrac{dI}{dt} = \boldsymbol{\beta} \odot S \odot I - \boldsymbol{\delta} \odot I + \mathrm{M}I \\ \dfrac{dR}{dt} = \boldsymbol{\delta} \odot I + \mathrm{M}R, \end{cases} \tag{2}$$

where for all $t \geq 0$*,* $S(t)$*,* $I(t)$ *and* $R(t)$ *are nonnegative vectors in* $\mathbb{R}^N$*.*

For instance, for each $1 \leq n \leq N$, $S_n(t)$ is the number of individuals of node n in compartment S. Standard results guarantee that the solution to Equation (2) is global, and converges to a fix point of the form $(S, 0, R)$, as $t \to \infty$ (Arino 2009). Moreover, the total population is preserved, that is $\sum_n (S_n(t) + I_n(t) + R_n(t))$ is constant. As for the diffusion dynamics, solutions of $d\mu/dt = \mathrm{M}\mu$ with initial condition μ_0 having a nonzero coordinate along $\tilde{\mu}_{\mathrm{M}}$ converge to $\tilde{\mu}_{\mathrm{M}}$, as $t \to \infty$. In particular, since the total population $S + I + R$ satisfies this equation, and its initial condition has a nonzero coordinate along $\tilde{\mu}_{\mathrm{M}}$ (according to the above, it equals $\sum_n (S_n(0) + I_n(0) + R_n(0))$, which is nonzero as $S(0)$, $I(0)$ and $R(0)$ have nonnegative coordinates), it converges to this stationary distribution, as $t \to \infty$.

We conclude this section by introducing the following two definitions, which help us formalise our setting.

[1] We adopt this terminology, for lack of a universally agreed term for these matrices between fields. Note that a diffusion matrix is the opposite of the Laplacian matrix of the corresponding weighted graph (Victor M Preciado, Jadbabaie, and Verghese 2013; Poignard, Pereira, and Pade 2018).

[2] This is possible if the graph is directed because we ask that, in that case, it is strongly connected.

Definition 3 (Configuration)**.** *We denote configuration, and write* $\mathcal{C} = (\mathrm{M},\, (\boldsymbol{\beta},\, \boldsymbol{\delta})\,,\, X_0)$*, a tuple consisting of a diffusion matrix* M*, epidemiological parameters gathered in* $\boldsymbol{\beta}$ *and* $\boldsymbol{\delta}$*, and an initial condition* $X_0 = (S_0,\, I_0,\, R_0) \in \mathbb{R}^{3N}$*. We write* $\mathfrak{C}$ *the set of configurations.*

Configurations contain all the necessary information to define the system of Equation (2). Therefore, we introduce the following notion of flow.

Definition 4 (Flows)**.** *We define the flow mapping* Φ *on the set of configurations* $\mathfrak{C}$ *by*[3]*:*

$$\begin{aligned} \Phi : \quad \mathfrak{C} &\to \quad \mathbf{C}\left(\mathbb{R}_+,\, \mathbb{R}^{3N}\right) \\ \mathcal{C} &\mapsto \qquad\qquad \Phi\left(\mathcal{C}\right) \end{aligned}$$

where, for each configuration $\mathcal{C} = (\mathrm{M},\, (\boldsymbol{\beta},\, \boldsymbol{\delta})\,,\, X_0)$*, for all* $t \geq 0$*,* $\Phi_t\left(\mathcal{C}\right)$ *is the value at time* t *of the solution of the differential Equation* (2)*, with initial condition* X_0*, that is* $\Phi_t\left(\mathcal{C}\right) = (S(t),\, I(t),\, R(t))$*.*

Slightly abusing notations, in the following, we sometimes write $\Phi(\mathrm{M})$ when $(\boldsymbol{\beta},\, \boldsymbol{\delta})$ and X_0 are fixed, so that the configuration only depends on the choice of the diffusion matrix. Moreover, for any typical time of diffusion $\tau > 0$, we write $\Phi^\tau = \Phi\left(\frac{\mathrm{M}}{\tau}\right)$, that is the flow obtained by replacing M by M/τ in Equation (2).

3.2 Network Reconstruction

We now introduce notions directly linked with network reconstruction: the observation matrix (Tyrcha and Hertz 2014), and the vectors of estimates of the reaction terms, and the derivatives. Let $(S,\, I,\, R)$ be the solution of Equation (2), for some configuration $\mathcal{C} = (\mathrm{M},\, (\boldsymbol{\beta},\, \boldsymbol{\delta})\,,\, X_0)$. We do not observe the whole trajectories, but only some samples of them. For some integer $K \geq 1$, let us then consider the sampling times $0 = t_0 < t_1 < t_2 < \ldots < t_K$. Let, for each node n, $\hat{S}_n(t_k)$ be the (possibly noisy) observation of compartment S in node n at time t_k, (and likewise for the other compartments). We can also estimate the vectors of derivatives, and of reaction terms, of Equation (2), from the observations, as is done in Shandilya and Timme (2011). For every $1 \leq k \leq K$, we define $\hat{\rho}_S(t_k) = -\boldsymbol{\beta} \odot \hat{S}(t_k) \cdot \hat{I}(t_k)$ the vector of reaction terms on S at time t_k, and $\hat{D}_S(t_k) = \left(\hat{S}(t_k) - \hat{S}(t_{k-1})\right)(t_k - t_{k-1})^{-1}$ the estimate of the derivative on S at time t_k. We do likewise for the other compartments.

Definition 5 (Observation matrix, derivatives and reaction terms)**.** *Let the observation matrix on* S *be*

$$\hat{O}_S = \begin{pmatrix} \hat{S}_1(t_1) & \ldots & \hat{S}_1(t_K) \\ \vdots & \ddots & \vdots \\ \hat{S}_N(t_1) & \ldots & \hat{S}_N(t_K) \end{pmatrix} \in \mathcal{M}_{N\times K}\left(\mathbb{R}\right).$$

[3] We write $\mathbf{C}\left(\mathbb{R}_+,\, \mathbb{R}^{3N}\right)$ the set of continuous functions from $\mathbb{R}_+$ to $\mathbb{R}^{3N}$.

Note likewise $\hat{O}_I$ the observations on I, and $\hat{O}_R$ those on R. Define finally the matrix by block $\hat{O}\left((t_k), \Phi(\mathrm{M})\right) = \left(\hat{O}_S, \hat{O}_I, \hat{O}_R\right) \in \mathcal{M}_{N\times 3K}(\mathbb{R})$. This is the observation matrix associated with the sampling times (t_k), and the flow $\Phi(\mathrm{M})$.

Likewise, we write $\hat{\rho}_S, \hat{D}_S \in \mathcal{M}_{N\times K}(\mathbb{R})$ the matrices of reaction terms (resp. derivatives) on S, and likewise for the other compartments. We finally define $\hat{\rho} = (\hat{\rho}_S, \hat{\rho}_I, \hat{\rho}_R) \in \mathcal{M}_{N\times 3K}(\mathbb{R})$ and $\hat{D} = \left(\hat{D}_S, \hat{D}_I, \hat{D}_R\right) \in \mathcal{M}_{N\times 3K}(\mathbb{R})$.

3.3 Symmetries

As we see in our study, symmetries of the trajectories have a crucial impact on the identifiability of the diffusion matrix. Let us therefore introduce the following related notions. We write $\mathfrak{S}_N$ the symmetric group of order N, and σ its elements, which are called permutations. We write $P(\sigma)$ the permutation matrix associated to the permutation σ. Then, for any $V \in \mathbb{R}^N$, $P(\sigma)V = V$ if, and only if, for every orbit of σ, for every i, j in this orbit, we have $V_i = V_j$. A vector $X = (S, I, R)$ is symmetric with respect to σ if $P(\sigma)S = S$, and likewise for I and R. This notion extends to groups of permutations, as follows. Let $\mathcal{H}$ be a subgroup of $\mathfrak{S}_N$, and define $\mathrm{Fix}(\mathcal{H})$ (Lang 2012) the space of vectors stable by $\mathcal{H}$, that is:

$$\mathrm{Fix}(\mathcal{H}) = \left\{V \in \mathbb{R}^N \,|\, \forall \sigma \in \mathcal{H}, P(\sigma)V = V\right\}.$$

For a set $\mathcal{S} \subset \mathbb{R}^N$, for $X = (S, I, R) \in \mathbb{R}^{3N}$, we write $X \in \mathcal{S}$ to mean that S, I and R belong to $\mathcal{S}$. Then, $X = (S, I, R)$ is said to be symmetric with respect to $\mathcal{H}$ if $X \in \mathrm{Fix}(\mathcal{H})$. This extends to flows by saying that a flow $(S, I, R) = \Phi(\mathcal{C})$ is symmetric with respect to $\mathcal{H}$ if, for all $t \geq 0$, we have $\Phi_t(\mathcal{C}) \in \mathrm{Fix}(\mathcal{H})$. Finally, we say that a configuration $\mathcal{C} = (\mathrm{M}, (\boldsymbol{\beta}, \boldsymbol{\delta}), X_0)$ is symmetric with respect to some permutation σ if, writing $P = P(\sigma)$, we have $\mathrm{M} = P\mathrm{M}P^{-1}$, $P\boldsymbol{\beta} = \boldsymbol{\beta}$, $P\boldsymbol{\delta} = \boldsymbol{\delta}$ and $PX_0 = X_0$. We then say σ is a configuration automorphism of $\mathcal{C}$, extending in a straigthforward way the notion of graph automorphism (Hell and Nesetril 2004). Indeed, if σ is an automorphism of $\mathcal{C}$, then it is in particular an automorphism of the underlying weighted graph, meaning that for all nodes $i, j \in \mathcal{N}$, the edges $i \rightsquigarrow j$ and $\sigma(i) \rightsquigarrow \sigma(j)$ have the same weight: $\mathrm{M}_{i,j} = \mathrm{M}_{\sigma(i),\sigma(j)}$. We write $\mathrm{Aut}(\mathcal{C})$ the group of configuration automorphisms of $\mathcal{C}$.

Finally define, for all $1 \leq i < j \leq N$, and for all $1 \leq k \leq N-1$, the redirection matrix

$$Z^{i,j,k} = E_{k,i} - E_{k,j} - E_{N,i} + E_{N,j},$$

where the $E_{r,s}$'s matrices are the vectors of the canonical basis of $\mathcal{M}_N(\mathbb{R})$. This matrix removes one unit of rate from the edge $j \rightsquigarrow k$, and adds one unit of rate on the edge $i \rightsquigarrow k$. It does the reverse with respect to the node N, taking one unit of rate from $i \rightsquigarrow N$ and adding it to $j \rightsquigarrow N$, in order to enforce the fact that the sums of the columns of $Z^{i,j,k}$ vanish, that is as much rate goes to each node than goes out. The matrix $Z^{i,j,k}$ is not a diffusion matrix (it has off-diagonal negative coefficients). However, thanks to the $-E_{N,i} + E_{N,j}$ term, adding a small enough multiple of $Z^{i,j,k}$ to a diffusion matrix, with non-zero entries at coordinates

$(k,\, j)$ and $(N,\, i)$, results in a diffusion matrix. For the sake of clarity, we use node N as a "pivot", but could have used any other node. Indeed, matrices of the form $Z^{i,j,k} - Z^{i,j,l}$ balance modifications on edges $i \rightsquigarrow k$ and $j \rightsquigarrow k$ by corresponding ones on edges $i \rightsquigarrow l$ and $j \rightsquigarrow l$, so that using them makes node N loose its specificity.

4 Well-Posedness, Diffusion Rate and Symmetries

We study, from a theoretical standpoint, the well-posedness of the reconstruction problem, (Section 4.1), the influence of the diffusion rate (Section 4.2), and the role played by symmetries (Section 4.3).

4.1 Well-Posedness of the Reconstruction Problem

We now show the diffusion matrix and initial condition generating the trajectories observed are almost everywhere unique, which implies that the reconstruction problem is almost everywhere well posed. We have the following characterisation of the set of diffusion matrices M which produce the same trajectories as M^* (see Appendix 7 for a proof, and likewise for future results).

Lemma 6 (Diffusion Matrices Generating the Same Trajectories)**.** *Let M^* be a diffusion matrix, and write $(S,\, I,\, R) = \Phi\left(\mathrm{M}^*\right)$. Then, every matrix $\mathrm{M} = \mathrm{M}^* + H$, such that first M is a diffusion matrix, and secondly such that for all $t \geq 0$, we have*[4] *$\Phi_t(\mathrm{M}) \in \ker H$, produces the same trajectories as M^*.*

As a result, provided the vector space spanned by the vectors $S(t)$, $I(t)$ and $R(t)$, for $t \geq 0$, is the whole space $\mathbb{R}^N$, then there is a unique diffusion matrix generating the trajectories (as the only H possible vanishes over the whole space, therefore vanishes). Therefore, a fundamental question governing the issue of the unicity, and consequently of the possibility of reconstruction, of the diffusion matrix is the existence of strict subspaces of $\mathbb{R}^N$ in which the trajectories evolve. This moreover gives us a seemingly easy to check criterion to evaluate if the diffusion matrix generating a given trajectory is unique, when there is no noise on the observations. Indeed, we can check if the observation matrix has rank N, which is sufficient to guarantee the uniqueness. However, this criterion is not practical, as we explain below. First however, we see that, often, the trajectories do generate the whole space.

Proposition 7 (Almost Everywhere Well-Posedness)**.** *Let $0 \leq t_1 < ... < t_N < \infty$ be a subdivision of the nonnegative real half-axis. Then, for almost every M, X_0, for all $\boldsymbol{\beta}$, $\boldsymbol{\delta}$, writing $\mathcal{C} = (\mathrm{M},\, (\boldsymbol{\beta},\, \boldsymbol{\delta})\,,\, X_0)$, the space generated by the samples of the trajectories at instants $t_1, ..., t_N$ (that is $\Phi_{t_1}(\mathcal{C}), \ldots, \Phi_{t_N}(\mathcal{C})$), is equal to $\mathbb{R}^N$.*

Therefore, linking with Lemma 6, this shows the reconstruction problem is almost everywhere well posed. This might give the impression the reconstruction problem is solved, for almost every M and X_0, when observations are not noisy. Indeed,

[4] As explained in Section 3.3, $\Phi_t(\mathrm{M}) \in \ker H$ means that $S(t)$, $I(t)$ and $R(t)$ belong to $\ker H$.

assume the space generated by the trajectories is the whole of $\mathbb{R}^N$. Then, the observation matrix $\hat{O}\left((t_k)\,,\,\Phi(\mathrm{M}^*)\right)$ has rank N. We therefore know the image of M^* on a basis, which fully determines it. However, the conditioning of the observation matrix is often poor in practise, so that reconstruction of M^* by extracting a basis is inefficient. Nonetheless, the fact the diffusion matrix is often unique means that, when running a reconstruction algorithm, we can have good hope it will succeed in finding a (at least relatively) good fit. We discuss it in the numerical simulations.

4.2 Diffusion Rate

Let us study the influence of the diffusion rate on the feasibility of the network reconstruction. One difficulty of the network reconstruction problem is the conditioning of the observation matrix (Definition 5), which may be poor. In particular, its numerical rank may be significantly lower than N, as observed also in Prasse and Van Mieghem (2020a). In our case, this may be partly due to the homogenisation performed by the diffusion dynamics. Indeed, given different epidemiological parameters, and different population sizes, the internal dynamics of the different nodes evolve differently. However, the diffusion dynamics tends to homogeneise each compartment, so that $S(t)$ tends to a vector proportional to the stationary distribution, $\tilde{\mu}_{\mathrm{M}}$, and likewise for $I(t)$ and $R(t)$. As a result, the diffusion dynamics tends to worsen the conditioning of a basis. This effect depends on the time-scale at which the diffusion dynamics occurs, with respect to that at which the reactions in each node occur. We first show, in the following Proposition 8, that when the typical time of evolution of the diffusion dynamics, τ, goes to 0, and in the presence of fixed epidemiological parameters, the trajectories tend to those of a scalar SIR system, multiplied by the stationary distribution. We express the coefficients of this scalar system in terms of the β_n's, the δ_n's and the stationary distribution.

Proposition 8 (Limit Trajectories for Diffusion Rate going to Infinity)**.** *Let* $\mathcal{C} = (\mathrm{M},\,(\boldsymbol{\beta},\,\boldsymbol{\delta})\,,\,X_0)$ *be a configuration, and assume the initial condition* X_0 *is such that* S_0*,* I_0 *and* R_0 *are proportional to the stationary distribution* $\tilde{\mu}_{\mathrm{M}}$*. Write* $(s,\,i,\,r)$ *the solutions of the scalar system*

$$\begin{cases} \dfrac{ds}{dt} = -\tilde{\beta} s i \\ \dfrac{di}{dt} = \tilde{\beta} s i - \tilde{\delta} i \\ \dfrac{dr}{dt} = \tilde{\delta} i, \end{cases}$$

with $s(0) = \sum_n S_n(0)$*, and likewise for* i *and* r*, and with*

$$\tilde{\beta} = \sum_n \beta_n \tilde{\mu}_{\mathrm{M}}(n)^2, \quad \textit{and} \quad \tilde{\delta} = \sum_n \delta_n \tilde{\mu}_{\mathrm{M}}(n).$$

Then, for any $T > 0$*,* $\Phi^\tau(\mathcal{C}) \to (s\tilde{\mu}_{\mathrm{M}},\,i\tilde{\mu}_{\mathrm{M}},\,r\tilde{\mu}_{\mathrm{M}})$*, as* $\tau \to 0$*, uniformly on* $t \in [0, T]$*.*

Proposition 8 is immediate when the stationary distribution $\tilde{\mu}_{\mathrm{M}}$ is uniform, as the trajectories are identically equal to the limit given in the statement. However, this

case is not common, as even the fact the diffusion matrix is symmetrical is not enough to ensure it has a uniform stationary distribution.

Let us note that, in a different perspective, but related to some extent in spirit, Prasse and Van Mieghem (2020b) have shown that the steady-state vector of a SIS epidemic on a network tends towards a limit proportional to the principal eigenvector of the adjacency matrix, when the basic reproduction number tends towards the epidemic threshold.

Then, from Proposition 8, we immediately have the following corollary which shows that a quick diffusion diminishes the numerical rank of the observation matrix. Let us recall that the numerical rank of a matrix with threshold η is the number of singular values of a matrix of modulus greater than η.

Corollary 9 (Numerical Rank of the Observation Matrix for Diffusion Rate going to Infinity)**.** *We make the same assumptions as in Proposition 8. Let, for some integer $K \geq 1$, $(t_k)_{1 \leq k \leq K}$ be a family of sample times. Let $\tau > 0$, and let us write $\hat{O}\left((t_k), \Phi^\tau(\mathrm{M})\right)$ the observation matrix associated with the t_k's, and the flow $\Phi^\tau(\mathrm{M})$. Then, the numerical rank, with threshold η, of the matrix $\hat{O}\left((t_k), \Phi^\tau(\mathrm{M})\right)$ goes to 1, as $\tau \to 0$ (but for a finite number of thresholds η[5]).*

4.3 Symmetries

Thanks to Lemma 6, we know that the unicity of M is linked to the dimension of the vector space spanned by the flow $\Phi(\mathcal{C})$. We now show that symmetries of the configuration are one cause which can lower this dimension, and therefore affect the well-posedness of the reconstruction problem. Indeed, when the trajectories have symmetries, then the space spanned by $\Phi(\mathrm{M})$ has dimension lower than N. Proposition 10 below shows that this happens whenever the diffusion matrix is symmetrical with respect to some group $\mathcal{H}$ (implication $2 \Rightarrow 1$), and that this is in fact an equivalence (implication $1 \Rightarrow 2$).

Proposition 10 (Networks Generating Symmetrical Trajectories)**.** *Let M be a diffusion matrix, $\boldsymbol{\beta}, \boldsymbol{\delta}$ be the vectors of epidemiological coefficients, and $\mathcal{H}$ be a subgroup of $\mathfrak{S}_N$. Assume that $\boldsymbol{\beta}$ and $\boldsymbol{\delta}$ are symmetric with respect to $\mathcal{H}$. Then, the following conditions are equivalent.*

1. *Symmetries of the Trajectories. For all $X_0 \in \mathrm{Fix}(\mathcal{H})$, the flow of $(\mathrm{M}, (\boldsymbol{\beta}, \boldsymbol{\delta}), X_0)$ is symmetric with respect to $\mathcal{H}$.*
2. *Symmetrical Generating Diffusion Matrix. There exists a diffusion matrix $\overline{\mathrm{M}}$ such that, for all $X_0 \in \mathrm{Fix}(\mathcal{H})$, first $\mathcal{H} \subset \mathrm{Aut}\left(\overline{\mathrm{M}}, (\boldsymbol{\beta}, \boldsymbol{\delta}), X_0\right)$, and second the flow of $\left(\overline{\mathrm{M}}, (\boldsymbol{\beta}, \boldsymbol{\delta}), X_0\right)$ equals the flow of $(\mathrm{M}, (\boldsymbol{\beta}, \boldsymbol{\delta}), X_0)$.*
3. *Stabilization by the Diffusion Matrix. The matrix M stabilizes $\mathrm{Fix}(\mathcal{H})$, that is $\mathrm{M}\mathrm{Fix}(\mathcal{H}) \subset \mathrm{Fix}(\mathcal{H})$.*

[5] These thresholds are the moduli of the singular values of some limiting matrix, see the proof of the result for details.

We now show that, in the spirit of Lemma 6, trajectories symmetrical with respect to $\mathcal{H}$ are generated by diffusion matrices which differ by a matrix Z vanishing on $\mathrm{Fix}(\mathcal{H})$. If the number of susceptible, infected and recovered individuals is the same at all times between several nodes, then redirecting the flows of individuals between these nodes does not change the trajectories. The Z matrices formalise this idea[6]. In particular, we show that Z matrices are generated by the redirection matrices. The nodes with identical values for S, I and R are those in the same orbits under $\mathcal{H}$ (Lang 2012), that is the nodes i and j such that, for some $\sigma \in \mathcal{H}$, we have $j = \sigma(i)$.

Lemma 11 (Flow Redirection within the Orbits)**.** *Under the same assumptions as in Proposition 10, let $\mathcal{H}$ be the biggest group of symmetries letting invariant the trajectories. Then, the affine space of matrices producing the same trajectories as* M *for every initial condition $X_0 \in \mathrm{Fix}(\mathcal{H})$ is exactly the subspace generated by the $Z^{i,j,k}$'s, for all i and j which are in the same orbit under $\mathcal{H}$. This space has dimension at least*

$$(N-1)(N - \#\{\textit{different trajectories}\}).$$

The dimension of this space is a lower bound on the dimension of the affine space of matrices generating the same trajectories as M. To summarize, given a diffusion matrix M, we have given an explicit description of a set of matrices giving the same trajectories as M. As a result, if the diffusion matrix we try to reconstruct gives symmetrical trajectories, and if we have an algorithm which gives us one solution of the reconstruction problem, then we are able to find many such matrices explicitly, though we cannot single the original M out. Note that this has consequences on the conditioning of the observation matrix. Indeed, its rank is then necessarily bounded by $\#\{\text{different trajectories}\}$. As such, if the configuration presents symmetries, then several singular values of the observation matrix will be zero, and in a neighbourhood of M as well, the numerical rank will be bounded by $\#\{\text{different trajectories}\} + \varepsilon$. This proves that the nearest a configuration is to a symmetrical configuration, the most difficult it is to reconstruct the diffusion matrix.

5 Numerical Simulations

We first describe our simulations set-up (Section 5.1), before studying numerically the influence of the diffusion rate (Section 5.2), and of the graph topology (Section 5.3). We then study the robustness of the reconstruction procedure to the presence of noise (Section 5.4). We conclude by studying a semi-real example (Section 5.5).

[6] In fact, the Z matrices, like the diffusion matrices, describe rates. However, as long as nodes have equal values, modifying the rates, or the flows going out of them, becomes equivalent.

5.1 Numerical Simulations Set-Up

Network Generation. For each numerical simulation, we start by generating a graph from a random graph generator. We use four random graphs, with different topologies: the Erdős-Rényi (Erdős and Rényi 1959) and the Waxman (Waxman 1988) graphs, which are rather connected graphs, and therefore relatively "close" to a complete graph, and the Relaxed Caveman (Fortunato 2010) and extended Barabási-Albert graphs (Barabási and Albert 2000), which are less connected, and exhibit a more clustered structure. In that sense, the diffusion dynamics is more constrained by these graphs, and we expect the reconstruction problems to be easier in that case. We study graphs of sizes ranging from $N = 20$ to $N = 130$. For the diffusion dynamics, we generate a diffusion matrix of the form $\mathrm{M}^* = \tau^{-1} \left(P - \mathrm{Id}_N\right)^T$, where P is a stochastic matrix, and $\tau > 0$ is the typical time of the diffusion dynamics[7]. The matrix P has nonzero entries corresponding to the edges of the graph. The values of these entries are drawn uniformly at random (and renormalised to ensure P is stochastic). As a consequence, the rate at which individuals leave each node is controlled by τ: for each node, it will take on average τ units of time for an individual to leave the node. The values of τ range from 10^{-3} to 2×10. For the reaction dynamics, the β_n's and δ_n's are drawn according to a lognormal law, with means $\bar{\beta}$ and $\bar{\delta}$ chosen as follows, and standard deviations $0.8\bar{\beta}$ and $0.8\bar{\delta}$. First, the mean $\bar{\delta}$ of the δ_n's is equal to 3×10^{-2} (meaning that individuals heal in 30 days on average). Then, we fix $\mathcal{R}_0 = 1.2$, and we choose $\bar{\beta}$ such that[8] $\mathcal{R}_0 = \bar{\beta} \left\|\tilde{\mu}_{\mathrm{M}^*}\right\|^2 / \bar{\delta}$.

Trajectories Simulations. Next, we simulate the ground truth trajectories. We first run the simulations on a deliberately long (from visual inspections) time interval $[0, 1000]$ (in days). We use a uniform time discretisation step of $(\Delta t)_{\text{groundtruth}} = 5 \times 10^{-3}$, and a Runge-Kutta discretisation scheme of order 4. Then, we determine an effective time interval $[0, T_\infty]$, with $T_\infty \leq 1000$, on which the dynamics truly unfolds, so as to avoid considering times for which it has already converged to its steady state[9]. The train set in which we sample the observations is $[0, T_{\text{train}}]$, with $T_{\text{train}} = 20\% \, T_\infty$. Finally, in each experiment, we use as initial condition $X_0 = (S(0), I(0), 0) = (s_0 \tilde{\mu}_{\mathrm{M}^*}, i_0 \tilde{\mu}_{\mathrm{M}^*}, 0)$, where $i_0 = 5\%$, and $s_0 = 1 - i_0$. As a result, the vector of initial susceptibles $S(0)$ is proportional to the stationary distribution of M^*, and likewise for $I(0)$ (and $R(0)$).

Reconstruction Algorithm. We sample the trajectories with various sample steps $(\Delta t)_{\text{sample}}$, ranging between 2×10^{-3} and 2×10^{-1}. We compute the recon-

[7] We use the notation Id_N to mean the identity matrix of order N.

[8] This ensures that, when the β_n's and the δ_n's have no variance, the basic reproduction number (Diekmann, J. A. P. Heesterbeek, and Roberts 2009) of the scalar system of Proposition 8 is equal to $\mathcal{R}_0$. The value $\mathcal{R}_0 = 1.2$ is slightly above the threshold 1, ensuring an epidemic does happen. Scaling the $\bar{\beta}$ like this ensures the dynamics has some degree of invariance with respect to the size of the network.

[9] To do this, for each trajectory, we determine a time T_∞ at which it has converged to its steady state, by asking that beyond T_∞, the total number of infected individuals is either less than 2% the size of the whole population, or less than 1/0.99 of its final value.

structed diffusion matrix by solving

$$\min_{\mathrm{M}\in\mathcal{M}_N(\mathbb{R})} \left\| \hat{D} - \hat{R} - \mathrm{M}\hat{O} \right\|_2 ,$$

$$\text{such that} \begin{cases} \mathrm{M}_{i,n} \geq 0,\, i \neq n, \\ \sum_{i=1}^{N} \mathrm{M}_{i,n} = 0 \quad \text{for each node} \quad n. \end{cases}$$

This is a convex optimisation problem. We solved it using the Python package CVXPY (Diamond and Boyd 2016; Agrawal et al. 2018). We write $\mathrm{M}_{\mathrm{rec}}$ the matrix obtained. Moreover, to truly enforce the fact $\mathrm{M}_{\mathrm{rec}}$ is a diffusion matrix (atoning for small numerical errors), we post-processed the matrix obtained by cancelling the off-diagonal negative coefficients, and enforcing that column sums vanish. Precisely, for every node n, we replaced the diagonal coefficient $\mathrm{M}_{\mathrm{rec}}(n,\, n)$ by $-\sum_{i=1, i\neq n}^{N} \mathrm{M}_{\mathrm{rec}}(i,\, n)$. The complexity of the algorithm is $O\left(N^2 3K\right)$, which is the standard cost for solving the regression.

Evaluation Metrics. To assess the reconstruction performance, we use two metrics. First, we use the area under the receiver operating characteristic curve (AUC) (Fawcett 2006) on the presence of edges, as Prasse and Van Mieghem (2020a). Secondly, we evaluate the prediction error, defined as follows. For known X_0 and epidemiological parameters, we define the prediction error as the norm of the difference between the trajectories computed with the true diffusion matrix M^*, and those computed with the reconstructed diffusion matrix $\mathrm{M}_{\mathrm{rec}}$, by

$$\textsc{PredictionError} = \frac{1}{N} \frac{1}{T_\infty - T_{\mathrm{train}}} \sum_{p=1}^{p_{\max}} \left\| \Phi_{t_p}(\mathrm{M}^*) - \Phi_{t_p}(\mathrm{M}_{\mathrm{rec}}) \right\|^2 (t_p - t_{p-1}) , \quad (3)$$

where $p_{\max} = \lfloor \frac{T_\infty - T_{\mathrm{train}}}{(\Delta t)_{\mathrm{groundtruth}}} \rfloor$, and (t_p) is the discretisation scheme used for the simulations, conducted on the test interval $[T_{\mathrm{train}}, T_\infty]$.

Let us now introduce the discrepancy error, which measures the discrepancy between the trajectories computed with a diffusion matrix M, and the limit trajectories of Proposition 8. Let M be a diffusion matrix, and let $\tilde{\mu}_{\mathrm{M}}$ be its stationary distribution. Let $(s,\, i,\, r)$ be the limit trajectory of Proposition 8, with values in $\mathbb{R}^3$. Then, $(s\tilde{\mu}_{\mathrm{M}},\, i\tilde{\mu}_{\mathrm{M}},\, r\tilde{\mu}_{\mathrm{M}})$ is a trajectory with values in $\mathbb{R}^{3N}$. We define the discrepancy error as the error between the solution of Equation (2), when the diffusion matrix is M/τ, and the trajectory $(s\tilde{\mu}_{\mathrm{M}},\, i\tilde{\mu}_{\mathrm{M}},\, r\tilde{\mu}_{\mathrm{M}})$. For (t_p) the discretisation scheme used for the simulations, and $p_{\max}$ the number of t_p's, it is defined by

$$\textsc{DiscrepancyError}(\tau) = \frac{1}{N} \frac{1}{T_\infty} \sum_{p=1}^{p_{\max}} \left\| \Phi_{t_p}(\frac{\mathrm{M}}{\tau}) - (s(t_p)\tilde{\mu}_{\mathrm{M}},\, i(t_p)\tilde{\mu}_{\mathrm{M}},\, r(t_p)\tilde{\mu}_{\mathrm{M}}) \right\|_2^2 (t_p - t_{p-1}) .$$

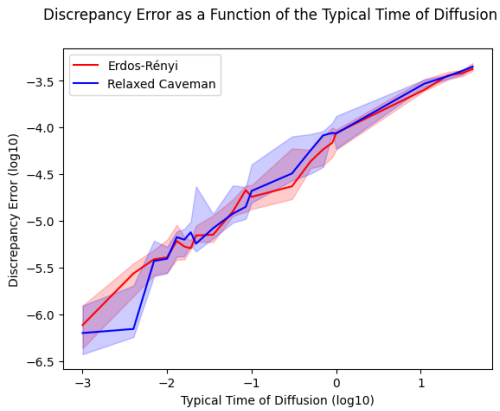

Figure 1: Discrepancy error as a function of the typical time of diffusion τ, for two random graphs of 50 nodes

Finally, we also consider in our numerical simulations the numerical rank of the observation matrix.

Plots Displayed. For each setting, we conduct several independent runs, and perform the reconstruction separately on each one of them, to average over the stochasticity of the choices. The plots we display are box plots, where the solid lines are the medians of values, and the shaded areas gather the [10%, 90%] intervals of values.

5.2 Influence of the Diffusion Rate

We now study numerically the influence of the diffusion rate, and we start by illustrating our theoretical results. First, on Figure 1, we display the discrepancy error as a function of the typical time of diffusion τ. The results are coherent with Proposition 8, as we see that it indeed goes to 0, as $\tau \to 0$. The convergence looks moreover almost exponential (as we use a log-log scale): this may be due to the fact it is driven by terms $\exp(\mathrm{M}t)$, restricted to a space where the biggest real parts of the eigenvalues of M are negative (see the proof for details). Second, on Figure 2, we show the numerical rank of the observation matrix as a function of τ . The results are coherent with Corollary 9, as we see the numerical rank gets lower and lower, as $\tau \to 0$. It is lower for the Erdős-Rényi graph, probably because it is denser than the Relaxed Caveman graph, and therefore is closer to some kind of average system, with more mixing between the nodes[10].

Let us now investigate the consequences the speed of diffusion has for the practi-

[10]In our simulations, the numerical rank reaches 5 at the lowest, but our implementation did not allow us to use yet lower values of τ, which would have allowed us to reach smaller numerical ranks. However, note that we used the Numpy defined threshold for the numerical rank: using a bigger threshold, equal to 10^{-6}, the numerical rank reached 2.

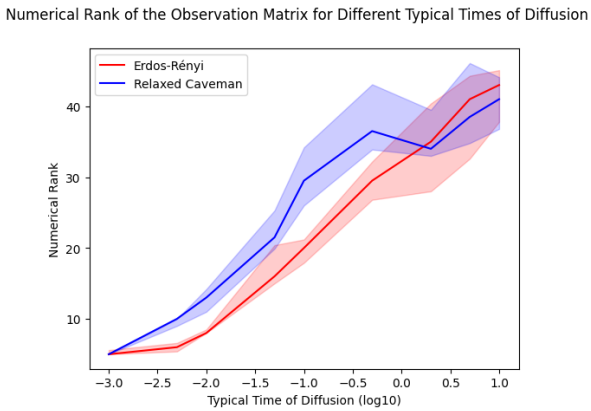

Figure 2: Numerical rank, of the observation matrix as a function of the typical time of diffusion τ, for two random graphs of 50 nodes, for a fixed family of sample times

cal reconstruction problem. We first show on Figure 3 the AUC as a function of the typical time of the diffusion dynamics τ, for a fixed sampling rate. The AUC increases as the typical time of the diffusion dynamics increases, as we expected. It is bigger for the Relaxed Caveman graph, which has "more structure" than the Erdős-Rényi one. Second, we study how increased sampling may help reconstruction for small typical times of diffusion. On Figure 4, we show a heatmap of the AUC, with different sampling steps $(\Delta t)_{\text{sample}} \in [5 \times 10^{-3}, 9 \times 10^{-2}]$, and typical times of diffusion $\tau \in [10^{-2}, 6]$, for a Relaxed Caveman graph of 50 nodes. The darker the color, the smaller the AUC is. On each row, we see colors get darker as we go to the right: this means that, for each fixed τ, the AUC deteriorates as the sampling step increases. On each column, we see colors get darker as we move to the top: this means that, for each sampling step, the AUC worsens as τ decreases. Therefore, reconstruction is indeed harder for quick diffusion dynamics, but increasing sampling may help counterbalance this.

5.3 Influence of the Network Topology

We now study numerically the influence of the network topology on the estimation and prediction problems. We present, on Figure 5, the AUC as a function of the number of nodes, for four types of random graphs. First, the AUC is often moderately good, and decreases as the number of nodes increases. Note that we deliberately considered a difficult scenario. Indeed, as all S, I and R components of the initial condition are proportional to the stationary distribution of the diffusion matrix, we only observe the diffusion indirectly, through the unequal evolution of the compartments in the different nodes, and their subsequent diffusion in the network. Using generic initial conditions makes it possible to observe directly the diffusion, so that the reconstruction problem is easier. Second, as expected, the

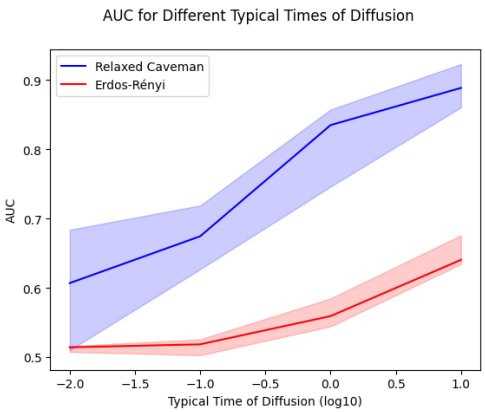

Figure 3: AUCs as a function of the typical time of diffusion τ, for two random graphs of size 50, for a fixed family of sample times

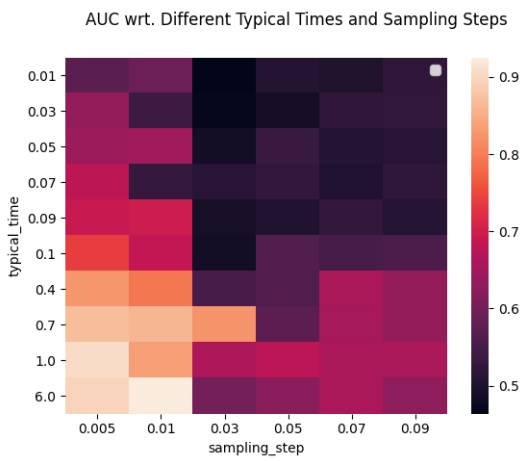

Figure 4: Heatmap of AUCs with respect to the typical time of diffusion τ (columns) and the sampling step $(\Delta t)_{\text{sample}}$ (lines), for a Relaxed Caveman graph of size 50

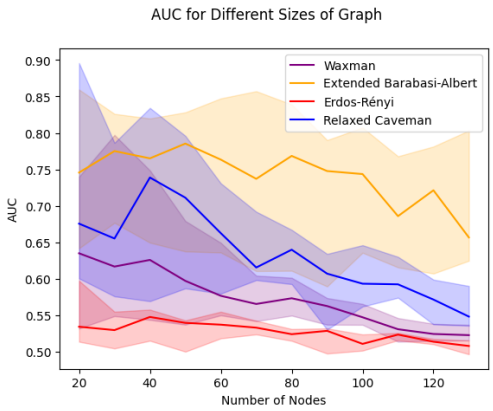

Figure 5: AUC on the Adjacency Matrix for Various Graphs and Sizes of Graphs

more structured the graph, the better the AUC. Indeed, it is best for the Barabási-Albert graph, and the second best is the Relaxed Caveman graph. The Waxman gaph, and above all the Erdős-Rényi one, which are denser, and where node values are mixed more, exhibit the worse AUCs. The dispersion around the median is greater for the "more structured graph": we believe it is due to the fact that small errors in crucial nodes may lead to huge consequences.

On Figure 6, we show the prediction error. We see the prediction errors in general are quite low, less than $10^{-3.5}$, and diminish with the number of nodes. Moreover, as the number of nodes increases, the Erdős-Rényi graph consistently exhibits the lowest error, followed by the Waxman graph. These results are consistent with each other, in the sense that it seems the more the graph has connections, the easiest it is to predict the future behaviour of the system (more edges, either through more nodes, or through the topology, in the case of the Erdős-Rényi graph). We see that they are opposite to the results for the AUCs: this tends to suggest that the more structured the topology, the easier it is to reconstruct the network, but the more mixing there is, the easiest it is to predict the future evolution of the system, which sounds reasonable enough.

5.4 Influence of Noise

We now study the influence of noise. We assume that the observation matrix is altered by an additive white Gaussian noise, such that, for each node n, for each $t \geq 0$, as far as the susceptible compartment is concerned, we observe

$$\hat{S}_n(t) = S_n(t) + \sigma \frac{(\Delta t)_{\text{sample}}}{10} \frac{\tilde{\mu}_{\text{M}}(n)}{3} E(t),$$

where σ is the noise standard deviation, and $E(t) \sim \mathcal{N}(0, 1)$ (with all the $E(t)$'s independent). We do likewise for the other compartments. As a result, for each node, for each compartment, the noise scales with the size of the node population,

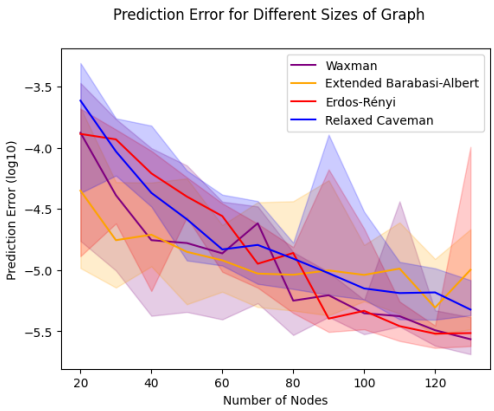

Figure 6: Prediction Error (log 10) for Various Graphs and Sizes of Graphs

	Barabási-Albert Graph	
σ	AUC	Prediction Error (log 10)
10^{-3}	0.74 [0.67, 0.78]	-4.8 [-4.9, -4.6]
10^{-2}	0.64 [0.59, 0.69]	-4.3 [-4.5, -4.3]
10^{-1}	0.63 [0.58, 0.67]	-4.2 [-4.4, -3.9]
1	0.56 [0.55, 0.57]	-4.1 [-4.2, -4.0]

Table 2: AUC and Prediction Error (log 10) on a Barabási-Albert graph of size 50, for different noise standard deviations. Median, and [10%, 90%] intervals of the results over the independant simulations, indicated.

renormalized by the number of compartments (3). On Table 2, we present the AUC and the logarithm of the prediction error, as a function of σ, for a Barabási-Albert graph of size 50. As far as the AUC is concerned, we see that noise degrades performances. However, signal is entirely lost, with AUCs close to 0.5, only for $\sigma = 1$, which shows some degree of robustness of the procedure. The prediction error is more robust to the presence of noise than the AUC, as it remains low even for $\sigma = 1$: this shows again that the prediction task is easier than the reconstruction task.

5.5 Semi-Real Data Example

Finally, we conducted simulations on a semi-real example. First, we selected 45 cities with airports in France, and created the graph of the flights between them: each node is a city, and there are edges between nodes n_1 and n_2 if there is one (or more) flight leading from n_1 to n_2. The graph is strongly connected. Then, we computed the relative sizes of the populations of the cities. Finally, we used gradient descent to compute a diffusion matrix whose stationary distribution was as close as possible to the vector of the relative sizes. The resulting network can be seen in Figure 7a. It was plotted with the graph-tool package (Peixoto 2014). The greater the value of the coordinate of the stationary distribution corresponding to a node,

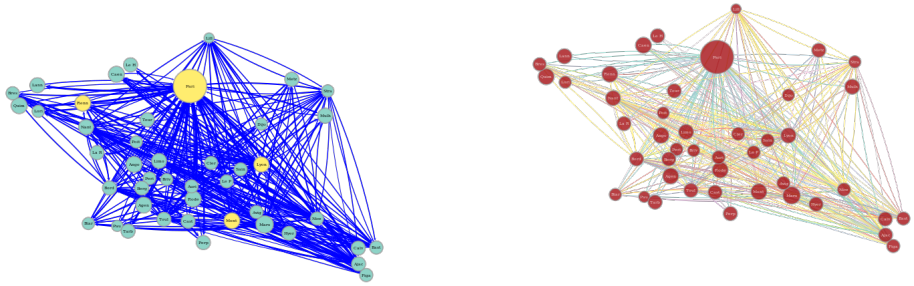

(a) Original network

(b) Relative errors for the reconstructed network

Figure 7: Original network, and relative errors for the reconstructed network. On the original network, cities discussed in the text are in yellow: Paris (top), Rennes (left), Lyon (middle right), Montpellier (bottom). On the reconstructed network, the edge colours show the size of the relative errors: small (green), middle (pink), large (yellow).

the bigger the node is: we logically see that the biggest node is Paris. The greater the value of the diffusion matrix corresponding to an edge, the bigger the edge size is. Then, we conducted our simulations as described in Section 5.1 (which means that the epidemic part of the example is synthetic). The AUC we obtained after training was 0.74, which is quite satisfying. We displayed in Figure 7b the relative errors between the original diffusion matrix, and the reconstructed one: for each non-diagonal entry, the relative error is $|\mathrm{M}^*(i,j) - \mathrm{M}_{\mathrm{rec}}(i,j)| \,/\, (\mathrm{M}^*(i,j) + \mathrm{M}_{\mathrm{rec}}(i,j))$. The edge colours are linked to the size of the relative errors: the smallest errors are in green, then the middle errors are in pink, and the largest errors are in yellow. In particular, wrongly inferring the presence of an edge leads to a big relative error. As expected, we see that most edges linked to Paris are in green: as Paris has a high connectivity, most edges inferred in the reconstruction indeed correspond to a true edge.

The relative errors for the reconstruction of edges $n \rightsquigarrow i$ are more correlated to the degree centrality of the destination nodes i (correlation: -0.60, meaning that relative errors on edges diminish when the centrality of destination nodes i increases), rather than the degree centrality of the origin nodes n (correlation: 0.45). This shows that what matters for reconstruction is the extent to which errors might propagate in the network. Indeed, if an edge goes to a node with high centrality, then an error on this edge will lead to errors further in the network. However, if this edge leaves a node with high centrality, but only goes to a node with low centrality, then errors on this edge will not have huge consequences for the overall reconstruction. The importance of this "error propagation" notion is further emphasised by

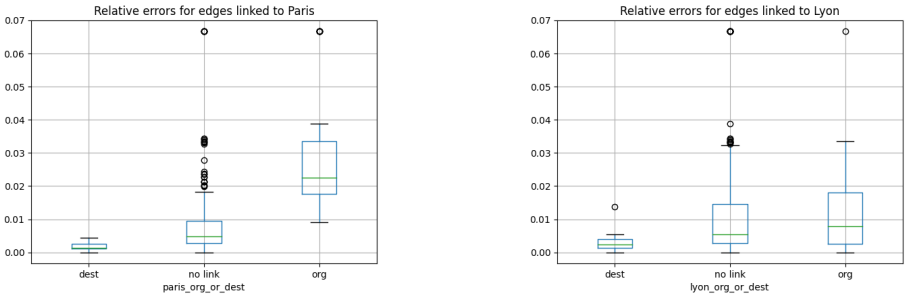

(a) Relative errors for Paris

(b) Relative errors for Lyon

Figure 8: Relative errors for high centrality nodes, depending on whether edges reach, or leave, the node. For comparison, the "no link" box gathers all edges not linked to the node.

noting that the same correlations, but computed with the stationary distributions of the nodes instead of the degree centralities, are weaker: -0.28 for the destination nodes, and 0.32 for the origin nodes. Finally, we see on Figure 8 and Figure 9 that the asymmetry between origin and destination is more pronounced for high centrality nodes, here Paris and Lyon, with centralities respectively equal to 1.55 and 1.05, than for low centrality nodes, like Montpellier and Rennes, both with 0.28 degree centralities. Edges reaching Paris and Lyon have lower errors than edges leaving them, while this is no longer the case for Montpellier and Rennes. Again, this shows that the relative errors are linked to the ability of errors to propagate into the network, as for low centrality nodes, errors will not have many consequences anyway.

6 Conclusions, future works

In this article, we have studied the reconstruction, and prediction, problems, for an epidemic reaction-diffusion. We have proved that for almost every network, the reconstruction problem is well-posed. Then, we have shown that the quicker the diffusion dynamics, the lower the numerical rank of the observation matrix, and the harder the reconstruction, but that increasing sampling helped reconstruct the network. Then, we have classified symmetrical networks generating the same trajectories. We showed numerically, on synthetic data constructed with random graph generators exhibiting different topologies, that reconstruction was easier for more "structured" topologies, and that the prediction problem could still be solved satisfyingly even when the network topology makes exact reconstruction difficult. Then, we studied the robustness of our procedure to noise. Finally, we studied a semi-real example.

Practically, we believe our work represents a step towards the possibility to disentangle internal versus external dynamics when observing reaction-diffusion spread-

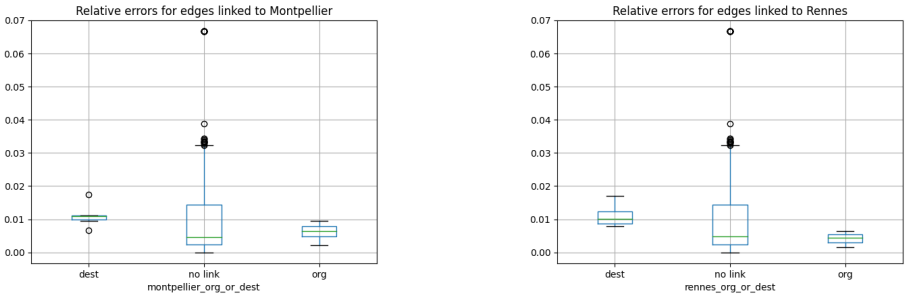

(a) Relative errors for Montpellier

(b) Relative errors for Rennes

Figure 9: Relative errors for low centrality nodes, depending on whether edges reach, or leave, the node. For comparison, the "no link" box gathers all edges not linked to the node.

ing processes in networks. This matters because the ability to distinguish the true causes driving an epidemic, for instance, is key when attempting to remedy it. Moreover, one crucial feature is the reconstruction of the diffusion dynamics structure: knowing which node (for instance, region or country) contributes more to the spread of an epidemic in which other node is an important information.

We have studied the case when the observations we have consist of all the trajectories in all the nodes. Other studies have considered partial observations (Nitzan, Casadiego, and Timme 2017; Ioannidis, Romero, and Giannakis 2018; Ioannidis, Y. Shen, and Giannakis 2019; Smiljanić et al. 2021), as for instance missing nodes (Tyrcha and Hertz 2014; Haehne et al. 2019), or coarser observations like the epidemic prevalence (Ma, Liu, and Van Mieghem 2019). To model this uncertainty, using a mixed probabilistic/deterministic generative model of the data, where the probabilistic part would cover the uncertainty, and incorporating it into a Bayesian reconstruction framework, as in Peixoto (2019), could prove valuable. This would be an interesting direction to further our work in.

Finally, in our work, reconstruction was hampered by bad conditioning of the observations matrix. This may be a consequence of the homogenisation performed by the diffusion matrix used. Other diffusive models, introducing more structure in the diffusion process, may prove more favourable to reconstruction, as for instance the hubs-attracting Laplacian introduced in Gambuzza, Frasca, and Estrada (2020).

7 Proofs for Section 4.1, Well-Posedness of the Reconstruction Problem

Lemma 6. Let $\mathrm{M} = \mathrm{M}^* + H$ be a diffusion matrix, such that for all $t \geq 0$, we have $S(t) \in \ker(H)$, $I(t) \in \ker(H)$ and $R(t) \in \ker(H)$. Let us check $(S,\, I,\, R) = \Phi(\mathrm{M}^*)$ is then a solution of Equation (2) with diffusion matrix equal to M. Indeed, for all $t \geq 0$, we have

$$\begin{aligned}\frac{dS}{dt}(t) &= -\boldsymbol{\beta} \odot S(t) \odot I(t) + \mathrm{M}^* S(t) \quad \text{by assumption}\\ &= -\boldsymbol{\beta} \odot S(t) \odot I(t) + \mathrm{M}^* S(t) + HS(t) \quad \text{as } S(t) \in \ker H\\ &= -\boldsymbol{\beta} \odot S(t) \odot I(t) + \mathrm{M} S(t).\end{aligned}$$

Likewise, I and R satisfy the corresponding equations, where diffusion is governed by M. Now, $(S,\, I,\, R)$ satisfies the differential equation Equation (2) with diffusion matrix M, and starts at the initial condition X_0. Therefore, by unicity of the solutions of this system, we have $(S,\, I,\, R) = \Phi(\mathrm{M})$. □

To prove Proposition 7, we first prove that the trajectories generated by a *linear* system often generate the whole space. Before doing this, we need the following technical lemmas.

Lemma 12 (Technical Result)**.** *For every integer $N \geq 1$, let $(\lambda_n)_{1\leq n\leq N}$ and $(t_k)_{1\leq k\leq N}$ be two families of distinct (within each family) real numbers. Then, for every $N \geq 1$, the following property holds true:*

$$\mathcal{P}(N) \;:\quad \forall 1 \;\leq\; n \;\leq\; N, \sum_{k=1}^{N} \mu_k e^{\lambda_n t_k} \;=\; 0 \;\Rightarrow\; (\forall 1 \;\leq\; k \;\leq\; N, \mu_k \;=\; 0).$$

Proof. We prove it by induction on N. The case $N = 1$ is immediate. Let $N \geq 2$, and let us show that if $\mathcal{P}(N-1)$ holds, then $\mathcal{P}(N)$ holds as well. Assume that for all $1 \leq n \leq N$, we have $\sum_{k=1}^{N} \mu_k e^{\lambda_n t_k} = 0$. Then, for all $1 \leq n \leq N$, we have

$$\sum_{k=1}^{N-1} \mu_k e^{\lambda_n (t_k - t_N)} + \mu_N = 0.$$

Let us consider the mapping:

$$g : \mathbb{R} \ni \lambda \mapsto \sum_{k=1}^{N-1} \mu_k e^{\lambda (t_k - t_N)} + \mu_N.$$

Then, g has N distinct roots (the λ_n's), therefore by Rolle's theorem, its derivative admits $N-1$ distinct roots. We therefore obtain $N-1$ values λ'_n such that, for all $1 \leq n \leq N-1$, $\lambda_n < \lambda'_n < \lambda_{n+1}$ and $\frac{dg}{d\lambda}(\lambda'_n) = 0$. As a result, for all $1 \leq n \leq N-1$, we have

$$0 = \frac{dg}{d\lambda}(\lambda'_n) = \sum_{k=1}^{N-1} \mu_k (t_k - t_N) e^{\lambda'_n (t_k - t_N)}.$$

By induction, for all $1 \leq k \leq N-1$, we have $\mu_k(t_k - t_N) = 0$, and therefore $\mu_k = 0$, as the t_k's are distinct. Then, $\mu_N = 0$ as well, hence the result. □

We need the following lemma. Though well-known, we could not locate a reference, so added it here for completeness.

Lemma 13 (Almost Every Diffusion Matrices has Distinct Eigenvalues)**.** *Almost every diffusion matrix has N distinct eigenvalues.*

Proof. Let $\mathcal{E}$ be the subset of diffusion matrices which do not have N distinct eigenvalues, and let us prove it has null measure. We know that $\mathcal{E}$ is the zero set of the discriminant Δ applied to the characteristic polynomial (Lang 2012), defined for every matrix A of order N by

$$F(A) = \Delta \circ \det(X\,\mathrm{Id} - A).$$

The set of diffusion matrices is contained in the linear subspace of matrices A satisfying $1_N^T A = 0$, which is of dimension $N^2 - N$. We equip it with the standard Lebesgue measure over $\mathbb{R}^{N^2-N}$.

Then, for any diffusion matrix $D \notin \mathcal{E}$, and any diffusion matrix M, $D + \lambda \mathrm{M}$ is in $\mathcal{E}$ only for a finite number of $\lambda \in \mathbb{R}$. Indeed, $\lambda \mapsto F(D+\lambda \mathrm{M}) = \Delta \circ \det(XId - D - \lambda \mathrm{M})$ is a polynomial function, so it is either zero or has a finite number of zeroes. But then it is nonzero at $\lambda = 0$, because $D \notin \mathcal{E}$. Therefore, the indicator function χ of $\mathcal{E}$ is zero almost everywhere on $\{D + \lambda \mathrm{M}, \lambda \in \mathbb{R}\}$, so it is also zero almost everywhere on $\{\mathrm{M} + \lambda D, \lambda \in \mathbb{R}\}$.

Let us finally fix some $D \notin \mathcal{E}$, and some vector space $\mathcal{H}$ such that $H \oplus \mathrm{Vect}(D) = \{A, 1_N^T A = 0\}$. Thanks to the Fubini-Tonelli theorem, we have

$$\int_{\mathbb{R}^{N^2-N}} \chi(A) dA = \int_{\mathcal{H}} \int_{\mathbb{R}} \chi(A + \lambda D) d\lambda dA = \int_{\mathcal{H}} 0 = 0.$$

Therefore, $\mathcal{E}$ has zero Lebesgue measure. □

Lemma 14 (Almost Everywhere Well-Posedness, linear case)**.** *Let $0 \leq t_1 < ... < t_N < \infty$ be a subdivision of the nonnegative real half-axis, $\mathrm{M} \in \mathcal{M}_N(\mathbb{R})$, and $y_0 \in \mathbb{R}^N$. Let y be the solution of the following differential equation:*

$$\begin{cases} \dfrac{dy}{dt} = \mathrm{M}y \\ y(0) = y_0. \end{cases} \tag{4}$$

Then, $(y(t_1), ..., y(t_N))$ is a basis of $\mathbb{R}^N$ for almost every M, y_0.

Proof. Let us prove the result for M and y_0 satisfying the additional assumptions that all the eigenvalues of M have multiplicity 1, and that every coordinate of y_0 in an eigenbasis of M is nonzero (note that as M has N distinct eigenvalues, the

associated subspaces are 1-dimensional, so the eigenbasis is unique up to permutation or scaling of the vectors). Thanks to Lemma 13, we will then have proved the result as stated, that is for almost every M, and also almost every y_0. (Indeed, the y_0's with at least one 0 coordinate live in a union of N hyperplanes $x_i = 0$, where x_i is i-th the coordinate in the eigenbasis, which has zero Lebesgue measure.).

Since y satisfies the linear equation $dy/dt = \mathrm{M}y$, we know that, for all $t \geq 0$, we have $y(t) = \exp(t\mathrm{M})y_0$. Let us write $\lambda_1, ..., \lambda_N$ the distinct eigenvalues of M, and (e_n) a corresponding eigenbasis. For all $t \geq 0$, we can decompose $y(t)$ along this eigenbasis. Let us write $y_1(t), \ldots, y_N(t)$ the corresponding coefficients so that, for all $t \geq 0$, we have $y(t) = \sum_n y_n(t)e_n$. By assumption, for every n, we have $y_n(0) \neq 0$. As a result, for every $t \geq 0$, we have

$$\begin{aligned} y(t) &= \exp(\mathrm{M}t)\, y_0 = \exp(\mathrm{M}t) \sum_n y_n(0)e_n \\ &= \sum_n \exp(tM)y_n(0)e_n = \sum_n \exp(t\lambda_n)y_n(0)e_n. \end{aligned}$$

We want to show that $(y(t_k))_{1\leq k\leq N}$ is a basis of $\mathbb{R}^N$. Let $\sum_k \mu_k y(t_k) = 0$ be a linear dependence relation. Since we have

$$\sum_{k=1}^N \mu_k y(t_k) = \sum_{k=1}^N \mu_k \sum_n e^{t_k\lambda_n} y_n(0)e_n = \sum_n y_n(0)e_n \sum_{k=1}^N \mu_k e^{t_k\lambda_n},$$

we know that, for all $n \in \mathcal{N}$, we have

$$\sum_{k=1}^N \mu_k e^{t_k\lambda_n} = 0,$$

using the unicity of coordinates in the basis $(e_n)_n$ and the fact that for all node n, we have $y_n(0) \neq 0$. We use Lemma 12 to conclude. □

We can now prove Proposition 7.

Proof. Let $K = S + I + R$ be the total population irrespective of infection status (for each node n, $K_n = S_n + I_n + R_n$ is the population of node n). By definition, for all $t \geq 0$, $K(t)$ is in the space generated by the trajectories. Then, K follows the differential equation

$$\begin{aligned} \frac{dK}{dt} &= \frac{dS}{dt} + \frac{dI}{dt} + \frac{dR}{dt} \\ &= -\boldsymbol{\beta} \odot S \odot I + \mathrm{M}S + \boldsymbol{\beta} \odot S \odot I - \boldsymbol{\delta} \odot I + \mathrm{M}I + \boldsymbol{\delta} \odot I + \mathrm{M}R \\ &= \mathrm{M}K. \end{aligned}$$

Using Lemma 14, we see that $(K(t_1), ..., K(t_N))$ generates $\mathbb{R}^N$ for almost every M, and $K(0) = S_0 + I_0 + R_0$, so for almost every M, S_0, I_0, R_0. As a result, for almost every M, $X_0 = (S_0, I_0, R_0)$, the space generated by the trajectories contains a family which generate $\mathbb{R}^N$. This proves our claim. □

8 Proofs for Section 4.2, analysis of the influence of the diffusion rate

Let us first prove the following result.

Lemma 15 (Trajectories Close to a Line for Infinitely Quick Diffusion Dynamics)**.** *Let us assume the initial condition X_0 is such that S_0, I_0 and R_0 are proportional to the stationary distribution.*

For every $\tau > 0$, let us write Φ^τ the solution of the system of Equation (2) where M *is replaced by* M/τ*, that is, for every $t \geq 0$, $\Phi^\tau_t = (S^\tau(t),\, I^\tau(t),\, R^\tau(t))$. Then, for all $T > 0$,*

$$\sup_{0 \leq t \leq T} \mathrm{d}\left(S^\tau(t),\, \mathbb{R}\tilde{\mu}_{\mathrm{M}}\right) \to 0,$$

when $\tau \to \infty$, and likewise for I^τ and R^τ.

The result extends to cases when X_0 is not proportional to the stationary distribution, only taking the supremum over some interval $[t(\tau), T]$, where $t(\tau)$ tends to 0, when $\tau \to 0$, and $t(\tau)$ represents the time it takes for the system to converge to the stationary distribution.

Proof. First, for all $\tau > 0$, and $t \geq 0$, we have

$$S^\tau(t) = \left(\sum_n S^\tau_n(t)\right) \tilde{\mu}_{\mathrm{M}} + \nu_\tau(t), \tag{5}$$

where $\nu_\tau(t)$ belongs to the set $\mathcal{H} = \left\{\nu \in \mathbb{R}^N \,|\, \sum_n \nu_n = 0\right\}$[11]. Moreover, $\nu_\tau(t)$ is bounded uniformly in $\tau > 0$ and $t \geq 0$, as all the $S^\tau(t)$'s are bounded by the total population, that is the sum of the coordinates of the initial condition X_0.

Then, for all $\tau > 0$, $t \mapsto \nu_\tau(t)$ is differentiable thanks to Equation (5) and, by differentiating Equation (5), we see ν_τ satisfies a differential equation of the form:

$$\frac{d\nu_\tau}{dt}(t) = \frac{\mathrm{M}}{\tau}\nu_\tau(t) + \gamma_\tau(t),$$

where γ_τ is a quantity depending on many things, but which is uniformly bounded in $\tau > 0$ and $t \geq 0$, again thanks to the fact that the $S^\tau(t)$'s, the $I^\tau(t)$'s and the $R^\tau(t)$'s are bounded by the total size of the population. Moreover, for all $\nu \in \mathbb{R}^N$, we have $\mathrm{M}\nu \in \mathcal{H}$, since the columns of M sum to 0. As a result, for all $\tau > 0$, and all $t \geq 0$, we have $\frac{d\nu_\tau}{dt}(t) \in \mathcal{H}$ (since $\mathcal{H}$ is a finite dimensional vector space, so derivatives of functions living on it stay in it), and $\frac{\mathrm{M}}{\tau}\nu_\tau(t) \in \mathcal{H}$ (by what precedes), so that $\gamma_\tau(t)$ also belongs to $\mathcal{H}$.

[11] This is a consequence of the decomposition $\mathbb{R}^N = \mathbb{R}\tilde{\mu}_{\mathrm{M}} \oplus \mathcal{H}$.

Finally, for all $\tau > 0$, and all $t \geq 0$, we have

$$\begin{aligned}\nu_\tau(t) &= \exp\left(\mathrm{M}\frac{t}{\tau}\right)\nu_\tau(0) + \int_0^t \exp\left(\mathrm{M}\frac{t-s}{\tau}\right)\gamma_\tau(s)\,ds \\ &= \int_0^t \exp\left(\mathrm{M}\frac{t-s}{\tau}\right)\gamma_\tau(s)\,ds,\end{aligned}$$

since $\nu_\tau(0) = 0$, as the initial condition is proportional to $\tilde{\mu}_\mathrm{M}$ by assumption. Let us now fix $\varepsilon > 0$. Let $B \subset \mathcal{H}$ be a ball such that, for all $\tau > 0$ and $t \geq 0$, we have $\gamma_\tau(t) \in B$. Since M only has eigenvalues with (strictly) negative eigenvalues on $\mathcal{H}$, we may find some threshold $u_\mathrm{min} > 0$ such that, for all $u \geq u_\mathrm{min}$, for all $\nu \in B$, we have

$$\|\exp(\mathrm{M}u)\,\nu\| < \varepsilon.$$

Moreover, there exists a constant $\kappa \geq 1$ such that, for all $u \geq 0$, for all $\nu \in B$, we have $\|\exp(\mathrm{M}u)\,\nu\| \leq \kappa$. Let us now consider $\tau \leq \frac{1}{u_\mathrm{min}}\frac{\kappa}{\varepsilon}$ (it is chosen so that, for $t - s \geq \frac{\varepsilon}{\kappa}$, we have $\frac{t-s}{\tau} \geq u_\mathrm{min}$). Therefore, for all $t \leq T$, we have

$$\begin{aligned}\|\nu_\tau(t)\| &\leq \int_0^t \left\|\exp\left(\mathrm{M}\frac{t-s}{\tau}\right)\gamma_\tau(s)\right\| ds \\ &= \int_0^{\frac{\varepsilon}{\kappa}} \left\|\exp\left(\mathrm{M}\frac{t-s}{\tau}\right)\gamma_\tau(s)\right\| ds + \int_{\frac{\varepsilon}{\kappa}}^T \left\|\exp\left(\mathrm{M}\frac{t-s}{\tau}\right)\gamma_\tau(s)\right\| ds \\ &\leq \frac{\varepsilon}{\kappa}\kappa + \int_{\frac{\varepsilon}{\kappa}}^T \varepsilon\,ds \leq \varepsilon + \varepsilon\left(T - \frac{\varepsilon}{\kappa}\right) \\ &\leq \varepsilon\,(1+T)\,.\end{aligned}$$

As a result, for all $\tau \leq \frac{1}{u_\mathrm{min}}\frac{\kappa}{\varepsilon}$, with u_min and κ chosen independently of τ, we have $\sup_{0\leq t\leq T}\|\nu_\tau(t)\| \leq \varepsilon\,(1+T)$. We have therefore proven that $\mathrm{d}\left(S^\tau(t), \mathbb{R}\tilde{\mu}_\mathrm{M}\right) \to 0$, as $\tau \to 0$. We would prove likewise the result for I^τ and R^τ, which concludes the proof. □

We can now prove Proposition 8.

Proof. Let $T > 0$. Now, let us write, for all $t \geq 0$, using the notations of the proof of Lemma 15, and $s_\tau(t) = \sum_n S_n^\tau(t)$,

$$S^\tau(t) = s_\tau(t)\tilde{\mu}_\mathrm{M} + \nu_\tau(t), \tag{6}$$

and likewise for I^τ and R^τ. Since S_0, I_0 and R_0 are proportional to the stationary distribution, we know, thanks to Lemma 15, that $\nu^\tau(t)$ tends towards 0, uniformly on each $[0, T]$, with $T \geq 0$. Since for all τ, S^τ, I^τ and R^τ are nonnegative, and bounded by the total population, the family of functions (s_τ, i_τ, r_τ), defined on $[0, T]$, has values in a bounded set of the continuous functions from $\mathbb{R}_+$ to $\mathbb{R}^3$, endowed with the infinity norm on each of s, i and r, that is $\|(s, i, r)\|_\infty = \max\left(\|s\|_\infty, \|i\|_\infty, \|r\|_\infty\right)$. Moreover since, for all $\tau \geq 0$, for all $0 \leq t \leq T$, we have

$$S^\tau(t) = S^\tau(0) - \int_0^t \boldsymbol{\beta} \odot S^\tau(s) \odot I^\tau(s) + \frac{\mathrm{M}}{\tau}S^\tau(s)\,ds,$$

we obtain, summing along the coordinates, and remembering that, for any vector V, $\mathrm{M}V \in \mathcal{H}$, so that the sum of the coordinates of $\mathrm{M}V$ is 0,

$$s_\tau(t) = s_\tau(0) - \sum_n \beta_n \tilde{\mu}_{\mathrm{M}}(n)^2 \int_0^t s_\tau(s) i_\tau(s)\, ds + \int_0^t \varepsilon_\tau(t)\, dt,$$

where $t \mapsto \varepsilon_\tau(t)$ is a continuous function which goes uniformly to 0 on $[0, T]$, as $\tau \to 0$ (we see this by developing the term $S^\tau \odot I^\tau = (s_\tau \tilde{\mu}_{\mathrm{M}} + \nu_\tau) \odot (i\tau \tilde{\mu}_{\mathrm{M}} + \tilde{\nu}_\tau)$, where $\tilde{\nu}_\tau$ is the equivalent of ν_τ for the coordinate I). As a result, s^τ is differential on $[0, T]$, its derivative satisfies

$$\frac{ds_\tau}{dt} = -\left(\sum_n \beta_n \tilde{\mu}_{\mathrm{M}}(n)^2\right) s_\tau(t) i_\tau(t) + \varepsilon_\tau(t),$$

and its derivative is threfore bounded on $[0, T]$, uniformly on τ. The same holds for i^τ and r^τ. Therefore, (s^τ, i^τ, r^τ) is equi-continuous. As a result, the family $((s^\tau, i^\tau, r^\tau))_{\tau \geq 0}$ is pre-compact (Sutherland 2004) in the Banach space of functions from $[0, T]$ to $\bar{\mathbb{R}}^3$, endowed with the infinity norm defined above, so that, provided it admits an unique adherence value, it converges towards this one.

Let us consider a converging subsequence, and still index it by τ, to simplify notations. As a result, the limit s satisfies

$$s(t) = s(0) + \sum_n \beta_n \tilde{\mu}_{\mathrm{M}}(n)^2 \int_0^t s(u) i(u)\, du,$$

and likewise for i and s. Moreover, for all $t \geq 0$, we know that $s_\tau(0) = \sum_n S^\tau(0) = \sum_n S_n(0)$ which does not depend on τ, therefore $s(0) = \sum_n S_n(0)$, and likewise for i_0 and r_0. Therefore, (s, i, r) is solution of the scalar system described in the statement of the Lemma, and by uniqueness of the solutions of this system, satisfying the initial condition (s_0, i_0, r_0), the tuple is uniquely defined. Therefore, the family of (s^τ, i^τ, r^τ)'s admits a unique adherence value, and converges towards this one. Plugging back into Equation (6), we see that $S^\tau \to s\tilde{\mu}_{\mathrm{M}}$, as $\tau \to 0$, uniformy on $[0, T]$, and likewise for I^τ and R^τ, which concludes the proof. □

Let us prove Corollary 9.

Proof. Applying the results of Proposition 8 with $T = t_K$, we know that the observation matrix writes

$$\hat{O}\left((t_k), \Phi^\tau(\mathrm{M})\right) = \tilde{\mu}_{\mathrm{M}} \otimes (s(t_1), \ldots, s(t_K), i(t_1), \ldots, i(t_K), r(t_1), \ldots, r(t_K)) + O\left(\varepsilon(\tau)\right), \quad (7)$$

as $\tau \to 0$, where $\varepsilon(\tau) \to 0$, when $\tau \to 0$. Indeed, using the notations of the proof of Proposition 8, we know that for each $1 \leq k \leq K$, the column $S(t_k)$ of the observation matrix (for instance), writes $S(t_k) = s(t_k)\tilde{\mu}_{\mathrm{M}} + \nu_\tau(t_k)$, and ν_τ

tends to 0, as $\tau \to 0$, uniformly on $[0, t_K]$. The first term of the right-hand-side of Equation (7) is of rank 1, as $s + i + r = 1$, identically. Let us write it A. Now, for every threshold η which is not the modulus of a singular value of A, the numerical rank with threshold η, that is the number of singular values greater than η, is continuous at A. The conclusion follows from the continuity of the singular values of the matrix. □

9 Proofs for Section 4.3, symmetries

Let us first show the effect of node-renumbering on the trajectories.

Lemma 16 (Node re-numbering)**.** *Let* $\mathcal{C} = (\mathrm{M}, (\boldsymbol{\beta}, \boldsymbol{\delta}), X_0)$ *be a configuration and* P *a permutation matrix. Then, for all* $t \geq 0$*, we have*

$$\Phi_t(P \cdot \mathcal{C}) = P \cdot \Phi_t(\mathcal{C}) = (PS(t), PI(t), PR(t)),$$

writing $(S(t), I(t), R(t)) = \Phi_t(\mathcal{C})$*, and* $P \cdot \mathcal{C} = \left(P\mathrm{M}P^{-1}, (P\boldsymbol{\beta}, P\boldsymbol{\delta}), PX_0\right)$.

This implies immediately that if P is the matrix of an automorphism of our configuration, then for all $t \geq 0$, we have $\Phi_t(P \cdot \mathcal{C}) = \Phi_t(\mathcal{C})$, and therefore $P \cdot \Phi_t(\mathrm{M}) = \Phi_t(\mathrm{M})$. In other words, if i and j are in a same orbit of P, then the trajectories at nodes i and j are the same: for all $t \geq 0$, $S_i(t) = S_j(t)$, and likewise for I and R.

Proof. Let us show that (PS, PI, PR) is a solution of the differential equation also satisfied by the flow $\Phi\left(P\mathrm{M}P^{-1}, (P\boldsymbol{\beta}, P\boldsymbol{\delta}), PX_0\right)$, which is enough to conclude by unicity of the solutions sharing the same initial condition. Let $1 \leq i \leq N$. Then, we have

$$\begin{aligned}
\frac{d}{dt}[PS]_i = \left[P\frac{dS}{dt}\right]_i &= \frac{dS_{\sigma(i)}}{dt} \\
&= -\beta_{\sigma(i)} S_{\sigma(i)} I_{\sigma(i)} + [MS]_{\sigma(i)} \\
&= -[P\beta]_i [PS]_i [PI]_i + [PMS]_i \\
&= -[P\beta]_i [PS]_i [PI]_i + [(PMP^{-1})(PS)]_i.
\end{aligned}$$

Therefore, we have

$$\frac{dPS}{dt} = -(P\boldsymbol{\beta}) \odot ((PS) \odot (PI)) + \left(P\mathrm{M}P^{-1}\right)(PS).$$

So PS satisfies the required equation, and I, R do as well, which we show using the same method, and which allows us to conclude. □

We can now prove Proposition 10.

Proof. Let us first prove 3) ⇒ 2). Let $\sigma \in \mathcal{H}$. For any $x \in \mathcal{H}$, we have

$$\begin{aligned}
P(\sigma)\mathrm{M}P(\sigma)^{-1}x &= P(\sigma)\mathrm{M}x \quad \text{as } x \in \mathrm{Fix}(\mathcal{H}) \\
&= \mathrm{M}x \quad \text{as } \mathrm{M}x \in \mathrm{Fix}(\mathcal{H}).
\end{aligned}$$

We now average the nodes which give the same trajectories, which is the standard method of averaging under a group action. Let

$$\overline{\mathrm{M}} = \frac{1}{\#\mathcal{H}} \sum_{\sigma \in \mathcal{H}} P(\sigma) \mathrm{M} P(\sigma)^{-1}.$$

We therefore obtain by construction that, for all $X_0 \in \mathrm{Fix}(\mathcal{H})$, we have $\mathcal{H} \subset \mathrm{Aut}(\overline{\mathrm{M}}, (\boldsymbol{\beta}, \boldsymbol{\delta}), X_0)$. The fact $\overline{\mathrm{M}}$ and M agree on $\mathrm{Fix}(\mathcal{H})$ is a direct consequence of the averaging. Now, since $\overline{\mathrm{M}}$ is symmetric with respect to $\mathcal{H}$, thanks to Lemma 16, we know that the trajectories it generates are also symmetric with respect to $\mathcal{H}$. As a result, they belong to $\mathrm{Fix}(\mathcal{H})$. Therefore, they also satisfy the differential equation with M, as we have just proven that M and $\overline{\mathrm{M}}$ agree on $\mathrm{Fix}(\mathcal{H})$.

Then, 2) $\Rightarrow$ 1) is a direct consequence of Lemma 16.

To prove 1) $\Rightarrow$ 3), let $S_0 \in \mathrm{Fix}(\mathcal{H})$, and let us show that $\mathrm{M}S_0 \in \mathrm{Fix}(\mathcal{H})$. Choose I_0 and R_0 such that $I_0 \in \mathrm{Fix}(\mathcal{H})$, and define $X_0 = (S_0,\, I_0,\, R_0)$. For every $\sigma \in \mathcal{H}$, for every node i, we have

$$[\mathrm{M}S(0)]_{\sigma(i)} = \frac{dS_{\sigma(i)}}{dt}(0) + \beta_{\sigma(i)} S_{\sigma(i)}(0) I_{\sigma(i)}(0).$$

Now, $\beta_\sigma(i) = \beta_i$ by assumption on the coefficients, and $S_{\sigma(i)}(0) I_{\sigma(i)}(0) = S_i(0) I_i(0)$ by assumption. Moreover, we have

$$\frac{dS_{\sigma(i)}}{dt}(0) = \lim_{t \to 0} \frac{S_{\sigma(i)}(t) - S_{\sigma_i}(0)}{t} = \lim_{t \to 0} \frac{S_i(t) - S_i(0)}{t} = \frac{dS_i}{dt}(0),$$

where the second equality is a consequence of the fact that trajectories remain in $\mathrm{Fix}(\mathcal{H})$. As a result, we have

$$[\mathrm{M}S(0)]_{\sigma(i)} = \frac{dS_i}{dt}(0) + \beta_i S_i(0) I_i(0) = [\mathrm{M}S(0)]_i.$$

Therefore, for every $\sigma \in \mathcal{H}$, we have $P(\sigma)\mathrm{M}S_0 = \mathrm{M}S_0$ so that, by definition, we have $\mathrm{M}S_0 \in \mathrm{Fix}(\mathcal{H})$.

□

Corollary 11. Let us first prove that $Z = \mathrm{M} - \overline{\mathrm{M}}$ vanishes on $\mathrm{Fix}(\mathcal{H})$. For all $X_0 \in \mathrm{Fix}(\mathcal{H})$, since M and $\overline{\mathrm{M}}$ produce the same trajectories, we have, for all $t \geq 0$,

$$\frac{dS}{dt} = -\boldsymbol{\beta} \odot S(t) \odot I(t) + \mathrm{M}S(t) = -\boldsymbol{\beta} \odot S(t) \odot I(t) + \mathrm{M}'S(t),$$

so that $ZS(t) = (\mathrm{M} - \mathrm{M}')\, S(t) = 0$. As a result, $ZS(0) = 0$. This is true for all $S(0) \in \mathrm{Fix}(\mathcal{H})$ (as $X_0 = (S_0,\, I_0,\, R_0)$ is arbitrary provided S_0, I_0 and R_0 all belong to $\mathrm{Fix}(\mathcal{H})$), so Z vanishes on $\mathrm{Fix}(\mathcal{H})$.

□

Corollary 11. This result is a particular case of the following Lemma 17, when we let $\mathcal{H}$ be the set of permutations under which the trajectories are invariant. In that case, the number of orbits of $\mathcal{H}$ is the number of different trajectories. □

Lemma 17 (Matrices vanishing on $\mathrm{Fix}(\mathcal{H})$)**.** *For any group of permutations $\mathcal{H}$, a basis of the space of matrices Z vanishing on $\mathrm{Fix}(\mathcal{H})$ is given by the $Z^{i,j,k}$'s, where i and j are in the same orbit under $\mathcal{H}$. Consequently, the dimension of this space is*

$$(N-1)\#\{\textit{orbits under } \mathcal{H}\}.$$

Proof. Let Z be such a matrix. As $Z = \mathrm{M} - \mathrm{M}'$ with M, M' diffusion matrices, the columns of Z have vanishing sums. Moreover, Z has to vanish on any vector fixed by $\mathcal{H}$. These vectors are precisely the $x \in \mathbb{R}^N$ such that $x_i = x_{\sigma(i)}$ for all $i \in \mathcal{N}$, and for all $\sigma \in \mathcal{H}$. Thus, they are the x's such that $E_{k,i}x = E_{k,\sigma(i)}x$ for every $i, k \in \mathcal{N}$, and $\sigma \in \mathcal{H}$. Therefore, $Z^{i,j,k}x = 0$ for all $x \in \mathrm{Fix}(\mathcal{H})$ when i, j, k satisfy the assumptions of the lemma. The $Z^{i,j,k}$'s are clearly linearly independent. Let us show that they generate the space of all Z's.

Let Z vanish on $Fix(\mathcal{H})$. We will make all of the coefficients of Z vanish by substracting multiples of $Z^{i,j,k}$s, which will prove that Z is indeed a linear combination of the $Z^{i,j,k}$s. Let $\mathcal{O} = \{i_1 < ... < i_m\}$ be an orbit of $\{1, ..., n\}$ of cardinal m under the action of $\mathcal{H}$.

Let us remark that for $1 \leq k \leq N-1$, $1 \leq l < m$, $Z^{i_l,i_{l+1},k}$ satisfies the conditions of the lemma and has its (k, i_l) coefficient equal to 1, its (k, i_{l+1}) coefficient equal to -1.

Therefore, $Z - Z_{k,i_1}Z^{i_1,i_2,k}$ has its (k, i_1) coefficient equaling zero, and its (k, i_2) coefficient equal to $Z_{k,i_2} + Z_{k,i_1}$, and aside from the last line (which we will ignore for the moment) these are the only coefficients changing.

Then, if $m \geq 3$, we can reiterate this by considering $Z - Z_{k,i_1}Z^{i_1,i_2,k} - (Z_{k,i_2} + Z_{i_1,k})Z^{i_2,i_3,k}$ and the obtained matrix will have the (k, i_2) coefficient vanishing and the (k, i_3) coefficient changing to $Z_{k,i_3} + Z_{k,i_2} + Z_{k,i_1}$, and the (k, i_1) coefficient is still 0.

We iterate this method exactly $m-1$ times to obtain Z'. By construction, Z' has each of the $(k, i_l), 1 \leq l \leq m$ coefficients vanishing except maybe the $l = m$ one, equaling $Z_{k,i_1} + ... + Z_{k,i_m}$.

But then this one is also zero. Indeed, if $(e_j)_j$ is the canonical basis, as $\sum_{l=1}^m e_{i_l} \in Fix(H)$, we have $Z' \sum_{l=1}^m e_{i_l} = 0$, and by looking the k-th coefficient, we obtain $Z'_{k,i_m} = Z_{k,i_1} + ... + Z_{k,i_m} = 0$.

We can then iterate this construction on every line except the last (meaning for $1 \leq k \leq N-1$) and every orbit to obtain Z''. By construction, every line of Z'' is zero, except maybe the last ($k = N$), but then as the columns of Z'' have a vanishing sum (as Z'' is a linear combination of Z and the $Z^{i,j,k}$), $Z'' = 0$. Thus, Z is in the space generated by the $Z^{i,j,k}$.

□

References

[Agr+18] Akshay Agrawal et al. "A rewriting system for convex optimization problems". In: *Journal of Control and Decision* 5.1 (2018), pp. 42–60 (cit. on p. 17).

[All+07] L. J. S. Allen et al. "Asymptotic Profiles of the Steady States for an SIS Epidemic Patch Model". In: *SIAM Journal of Applied Mathematics* 67 (5 2007), pp. 1283–1309 (cit. on pp. 4, 5).

[Ang+17] M. T. Angulo et al. "Fundamental limitations of network reconstruction from temporal data". In: *Journal of the Royal Society Interface* 14 (2017) (cit. on p. 5).

[Ari09] Julien Arino. "Diseases in Metapopulations". In: *Modeling and Dynamics of Infectious Diseases* (2009), pp. 64–122 (cit. on pp. 3, 8, 9).

[Ari17] Julien Arino. "Spatio-temporal spread of infectious pathogens of humans". In: *Infectious Disease Modelling* (2 2017), pp. 218–228 (cit. on pp. 4, 5).

[Asl+20] Malbor Asllani et al. "Dynamics impose limits to detectability of network structure". In: *New Journal of Physics* 2 (2020) (cit. on pp. 3, 5).

[BA00] A. L. Barabási and R. Albert. "Topology of evolving networks: local events and universality". In: *Physical review letters* 85 (24 2000) (cit. on p. 16).

[BB13] B. Barzel and A.-L. Barabàsi. "Network link prediction by global silencing of indirect correlations". In: *Natural Biotechnologies* 31 (2013), pp. 720–725 (cit. on p. 6).

[BD01] Fred Brauer and P. van den Driessche. "Models for transmission of disease with immigration of infectives". In: *Mathematical Biosciences* 171 (2 June 2001), pp. 143–154 (cit. on pp. 3, 5).

[BIM19] Alfredo Braunstein, Alessandro Ingrosso, and Anna Paola Muntoni. "Network reconstruction from infection cascades". In: *Journal of the Royal Society Interface* 16 (2019) (cit. on p. 7).

[BKT11] F. van Bussel, B. Kriener, and Marc Timme. "Inferring synaptic connectivity from spatio-temporal spike patterns". In: *Frontiers in Computational Neurosciences* 5 (3 Feb. 2011) (cit. on p. 6).

[BR08] M. Broom and Rychtář. "An analysis of the fixation probability of a mutant on special classes of non-directed graphs". In: *Proceedings of the Royal Society A* 464 (2008), pp. 2609–2627 (cit. on p. 7).

[Cas+17] Jose Casadiego et al. "Model-free inference of direct network interactions from nonlinear collective dynamics". In: *Nature Communications* (2017) (cit. on p. 6).

[DB16] Steven Diamond and Stephen Boyd. "CVXPY: A Python-embedded modeling language for convex optimization". In: *Journal of Machine Learning Research* 17.83 (2016), pp. 1–5 (cit. on p. 17).

[DHB12] Odo Diekmann, Hans Heesterbeek, and Tom Britton. *Mathematical Tools for Understanding Infectious Disease Dynamics*. Princeton series in theoretical and computational biology. 2012 (cit. on pp. 3–5).

[DHR09] Odo Diekmann, J. A. P. Heesterbeek, and M. G. Roberts. "The construction of next-generation matrices for compartmental epidemic models". In: *Journal of The Royal Society* (2009). DOI: 10.1098/rsif.2009.0386 (cit. on pp. 5, 16).

[Don+15] Xiaowen Dong et al. "Laplacian matrix learning for smooth graph signal representation". In: *2015 IEEE International Conference on Acoustics, Speech and Signal Processing (ICASSP)* (2015), pp. 3736–3740 (cit. on p. 3).

[Dur10] Rick Durrett. "Some features of the spread of epidemics and information on a random graph". In: *Proceedings of the National Academy of Sciences* 107.10 (2010), pp. 4491–4498. ISSN: 0027-8424. DOI: 10.1073/pnas.0914402107. eprint: https://www.pnas.org/content/107/10/4491.full.pdf. URL: https://www.pnas.org/content/107/10/4491 (cit. on p. 7).

[EF21] Clive Emary and Hugo Fort. "Markets as ecological networks: inferring interactions and identifying communities". In: *Journal of Complex Networks* 9.2 (Aug. 2021). cnab022. ISSN: 2051-1329. DOI: 10.1093/comnet/cnab022. eprint: https://academic.oup.com/comnet/article-pdf/9/2/cnab022/39868832/cnab022.pdf. URL: https://doi.org/10.1093/comnet/cnab022 (cit. on p. 3).

[ER59] P. Erdős and A. Rényi. "On Random Graphs". In: *Publicationes Mathematicae* 6 (1959), pp. 290–297 (cit. on p. 16).

[Faw06] Tom Fawcett. "An introduction to ROC analysis". In: *Pattern Recognition Letters* 27.8 (2006). ROC Analysis in Pattern Recognition, pp. 861–874. ISSN: 0167-8655. DOI: https://doi.org/10.1016/j.patrec.2005.10.010. URL: https://www.sciencedirect.com/science/article/pii/S016786550500303X (cit. on p. 17).

[FH08] L. Filliger and M.-O. Hongler. *Lumping complex networks*. 2008 (cit. on p. 7).

[For10] Santo Fortunato. "Community Detection in Graphs". In: *Physics Reports* 486 (3–5 Feb. 2010), pp. 75–174 (cit. on p. 16).

[Gar+03] T. Gardner et al. "Inferring Genetic Networks and Identifying Compound Mode of Action via Expression Profiling". In: *Science* 301 (5629 July 2003), pp. 102–105 (cit. on pp. 3, 5, 6).

[GFE20] Lucia Valentina Gambuzza, Mattia Frasca, and Ernesto Estrada. "Hubs-attracting Laplacian and Related Synchronization on Networks". In: *SIAM Journal on Applied Dynamical Systems* 19.2 (2020), pp. 1057–1079. DOI: 10.1137/19M1287663. eprint: https://doi.org/10.1137/19M1287663. URL: https://doi.org/10.1137/19M1287663 (cit. on p. 25).

[GMT05] A. Ganesh, L. Massoulié, and D. Towsley. "The effect of network topology on the spread of epidemics". In: *Proceedings IEEE 24th Annual*

Joint Conference of the IEEE Computer and Communications Societies. 2 (2005), 1455–1466 vol. 2 (cit. on p. 7).

[GS06] Martin Golubitsky and Ian Stewart. "Nonlinear Dynamics of Networks: the Groupoid Formalism". In: *Bulletin (New Series) of the American Mathematical Society* 43 (3 July 2006), pp. 305–364 (cit. on p. 7).

[Hae+19] Hauke Haehne et al. "Detecting Hidden Units and Network Size from Perceptible Dynamics". In: *Phys. Rev. Lett.* 122 (15 Apr. 2019), p. 158301. DOI: 10.1103/PhysRevLett.122.158301. URL: https://link.aps.org/doi/10.1103/PhysRevLett.122.158301 (cit. on p. 25).

[HG97] I. A. Hanski and M.E. Gilpin. *Metapopulation Biology: Ecology, Genetics, and Evolution.* Academic Press, 1997 (cit. on p. 3).

[HN04] P. Hell and J. Nesetril. *Graphs and Homomorphisms.* Oxford Lecture Series in Mathematics and Its Applications. OUP Oxford, 2004. ISBN: 9780198528173. URL: https://books.google.fr/books?id=bJXWV-qK7kYC (cit. on p. 11).

[IRG18] Vassilis N. Ioannidis, Daniel Romero, and Georgios B. Giannakis. "Inference of Spatio-Temporal Functions Over Graphs via Multikernel Kriged Kalman Filtering". In: *IEEE Transactions on Signal Processing* 66.12 (2018), pp. 3228–3239. DOI: 10.1109/TSP.2018.2827328 (cit. on p. 25).

[ISG19] Vassilis N. Ioannidis, Yanning Shen, and Georgios B. Giannakis. "Semi-Blind Inference of Topologies and Dynamical Processes Over Dynamic Graphs". In: *IEEE Transactions on Signal Processing* 67 (9 May 2019) (cit. on p. 25).

[KM27] William Ogilvy Kermack and A.G. McKendrick. "A contribution to the mathematical theory of epidemics". In: *Journal of The Royal Society* (1927) (cit. on p. 3).

[KS08] G. Karlebach and R. Shamir. "Modelling and analysis of gene regulatory networks". In: *Nature Review of Molecular Cellular Biology* 9 (2008), pp. 770–780 (cit. on p. 3).

[Lan12] S. Lang. *Algebra.* Graduate Texts in Mathematics. Springer New York, 2012. ISBN: 9781461265511. URL: https://books.google.fr/books?id=Yt7LnQEACAAJ (cit. on pp. 11, 15, 27).

[Le +19] Batiste Le Bars et al. "Learning Laplacian Matrix from Bandlimited Graph Signals". In: *ICASSP 2019 - 2019 IEEE International Conference on Acoustics, Speech and Signal Processing (ICASSP).* 2019, pp. 2937–2941. DOI: 10.1109/ICASSP.2019.8682769 (cit. on p. 3).

[Li+17] Jingwen Li et al. "Universal data-based method for reconstructing complex networks with binary-state dynamics". In: *Physical Review E* 95 (2017) (cit. on p. 6).

[Ma+15] Long Ma, Xiao Han, et al. "Efficient Reconstruction of Heterogeneous Networks from Time Series via Compressed Sensing". In: *PLoS ONE* 10 (11 2015) (cit. on p. 6).

[Man+16] N. M. Mangan et al. "Inferring biological networks by sparse identification of nonlinear dynamics". In: *IEEE Transactions on Molecular,*

Biological and Multi-Scale Communications 2 (2016), pp. 52–63 (cit. on p. 6).

[Mey00] Carl D. Meyer. *Matrix Analysis and Applied Linear Algebra*. Society for Industrial and Applied Mathematics Philadelphia, PA, USA, 2000 (cit. on p. 9).

[MLV19] Long Ma, Qiang Liu, and Piet Van Mieghem. "Inferring network properties based on the epidemic prevalence". In: *Applied Network Science* 4 (93 2019) (cit. on pp. 6, 25).

[MPF05] V. Makarov, F. Panetsos, and O. de Feo. "A method for determining neural connectivity and inferring the underlying networks dynamics using extracellular spike recordings". In: *Journal of Neurosciences Methods* 144 (2 2005), pp. 265–279 (cit. on p. 6).

[MSA08] Ben D. MacArthur, Rubén J. Sánchez-García, and James W. Anderson. "Symmetry in complex networks". In: *Discreted Applied Mathematics* 156 (2008), pp. 3525–3531 (cit. on p. 7).

[NCT17] Mor Nitzan, Jose Casadiego, and Marc Timme. "Revealing physical interaction networks from statistics of collective dynamics". In: *Science Advances* 3 (Feb. 2017) (cit. on p. 25).

[NPP16] Cameron Nowzari, Victor M. Preciado, and George J. Pappas. "Analysis and Control of Epidemics: A survey of spreading processes on complex networks". In: *IEEE Control Systems Magazine* (2016) (cit. on pp. 3, 5).

[NWS02] M. E. J. Newman, D. J. Watts, and S. H. Strogatz. "Random graphs of social networks". In: *Proc. Natl. Acad. Sci. USA* 99 (1 2002), pp. 2566–2572 (cit. on p. 3).

[Pas+15] R. Pastor-Satorra et al. "Epidemic processes in complex networks". In: *Review of Modern Physics* 87 (3 2015), pp. 925–979 (cit. on p. 3).

[PDV21] Bastian Prasse, Karel Devriendt, and Piet Van Mieghem. "Clustering for epidemics on networks: a geometric approach". In: *preprint* (2021) (cit. on p. 7).

[Pec+14] Louis M. Pecora et al. "Cluster synchronization and isolated desynchronization in complex networks with symmetries". In: *Nature Communications* 5 (2014) (cit. on p. 7).

[Pei14] Tiago P. Peixoto. "The graph-tool python library". In: *figshare* (2014). DOI: 10.6084/m9.figshare.1164194. URL: http://figshare.com/articles/graph_tool/1164194 (visited on 09/10/2014) (cit. on p. 22).

[Pei19] Tiago P. Peixoto. "Network Reconstruction and Community Detection from Dynamics". In: *Physical Review Letters* 123 (2019) (cit. on pp. 7, 25).

[Per+17] Domenico Perfido et al. "Towards Sustainable Water Networks: Automated Fault Detection and Diagnosis". In: *The International Journal of Entrepreneurship and Sustainability Issues* 4 (3 Mar. 2017) (cit. on p. 3).

[PJV13] Victor M Preciado, Ali Jadbabaie, and George C Verghese. "Structural analysis of Laplacian spectral properties of large-scale networks". In:

IEEE Transactions on Automatic Control 58.9 (2013), pp. 2338–2343 (cit. on p. 9).

[PPP18] Camille Poignard, Tiago Pereira, and Jan Philipp Pade. "Spectra of Laplacian Matrices of Weighted Graphs: Structural Genericity Properties". In: *SIAM Journal on Applied Mathematics* 78.1 (2018), pp. 372–394. DOI: 10.1137/17M1124474. eprint: https://doi.org/10.1137/17M1124474. URL: https://doi.org/10.1137/17M1124474 (cit. on p. 9).

[PV01] R. Pastor-Satorras and A. Vespignani. "Epidemic spreading in scale-free networks". In: *Physical Review Letter* 86 (14 2001) (cit. on p. 3).

[PV04] R. Pastor-Satorras and A. Vespignani. *Internet: structure et évolution*. Belin, 2004 (cit. on p. 3).

[PV20a] Bastian Prasse and Piet Van Mieghem. "Network Reconstruction and Prediction of Epidemic Outbreaks for General Group-Based Compartmental Epidemic Models". In: *IEEE Transactions on Network Science and Engineering* 7 (4 2020) (cit. on pp. 3, 6, 8, 13, 17).

[PV20b] Bastian Prasse and Piet Van Mieghem. "Time-dependent solution of the NIMFA equations around the epidemic threshold". In: *Journal of Mathematical Biology* 81 (2020), pp. 1299–1355 (cit. on p. 14).

[Qui+11] C. J. Quinn et al. "Estimating the directed information to infer causal relationships in ensemble neural spike train recordings". In: *Journal of Computational Neurosciences* 30 (2011), pp. 17–44 (cit. on p. 6).

[RD21] Gemma Rosell-Tarragó and Albert Díaz-Guilera. "Quasi-symmetries in complex networks: a dynamical model approach". In: *Journal of Complex Networks* 9.3 (Aug. 2021). cnab025. ISSN: 2051-1329. DOI: 10.1093/comnet/cnab025. eprint: https://academic.oup.com/comnet/article-pdf/9/3/cnab025/40084975/cnab025.pdf. URL: https://doi.org/10.1093/comnet/cnab025 (cit. on p. 7).

[SB93] J. Stoer and R. Burlisch. *Introduction to Numerical Analysis*. New York: Springer, 1993 (cit. on p. 6).

[SBL19] Stefania Sardellitti, Sergio Barbarossa, and Paolo Di Lorenzo. "Graph Topology Inference Based on Sparsifying Transform Learning". In: *IEEE Transactions on Signal Processing* 67.7 (Apr. 2019), pp. 1712–1727. DOI: 10.1109/TSP.2019.2896229. arXiv: 1806.01701 [eess.SP] (cit. on p. 3).

[SD20] Anastasiya Salova and Raissa M. D'Souza. "Decoupled synchronized states in networks of linearly coupled limit cycle oscillators". In: *Physical Review Research* 2 (4 2020) (cit. on p. 7).

[She+14] Zhesi Shen et al. "Reconstructing propagation networks with natural diversity and identifying hidden sources". In: *Nature Communications* 5 (2014) (cit. on p. 6).

[Smi+21] Jelena Smiljanić et al. "Mapping flows on weighted and directed networks with incomplete observations". In: *Journal of Complex Networks* 9.6 (Dec. 2021). cnab044. ISSN: 2051-1329. DOI: 10.1093/comnet/cnab044. eprint: https://academic.oup.com/comnet/article-

pdf/9/6/cnab044/43291274/cnab044.pdf. URL: https://doi.org/10.1093/comnet/cnab044 (cit. on p. 25).

[Sor+22] David Soriano-Paños et al. "Modeling Communicable Diseases, Human Mobility, and Epidemics: A Review". In: *Annalen der Physik* n/a.n/a (2022), p. 2100482. DOI: https://doi.org/10.1002/andp.202100482. eprint: https://onlinelibrary.wiley.com/doi/pdf/10.1002/andp.202100482. URL: https://onlinelibrary.wiley.com/doi/abs/10.1002/andp.202100482 (cit. on p. 4).

[ST11] Srinivas Gorur Shandilya and Marc Timme. "Inferring network topology from complex dynamics". In: *New Journal of Physics* 13 (2011) (cit. on pp. 3, 6, 10).

[STK11] P. L. Simon, M. Taylor, and I. Z. Kiss. "Exact epidemic models on graphs using graph-automorphism driven lumping". In: *Journal of Mathematical Biology* 62 (4 2011), pp. 479–508 (cit. on p. 7).

[Sur+19] Francesco Vicenzo Surano et al. "Backbone reconstruction in temporal networks from epidemic data". In: *Physical Review E* 100 (2019) (cit. on p. 7).

[Sut04] Wilson Alexander Sutherland. *Introduction to Metric and Topological Spaces*. Oxford University Press, 2004 (cit. on p. 31).

[TC14] Marc Timme and Jose Casadiego. "Revealing networks from dynamics: an introduction". In: *Journal of Physics A: Mathematical and Theoretical* 47 (2014) (cit. on pp. 3, 5).

[TH14] Joanna Tyrcha and John Hertz. "Network Inference with Hidden Units". In: *Mathematical Biosciences and Engineering* 11 (1 Feb. 2014), pp. 149–165 (cit. on pp. 6, 10, 25).

[Tie+15] Joseph H. Tien et al. "Disease invasion on community networks with environmental pathogen movement". In: *Journal of Mathematical Biology* 70 (2015), pp. 1065–1092 (cit. on pp. 4, 5).

[TOM19] Natascia Tamburello, Brian O. Ma, and Isabelle M. Côté. "From individual movement behaviour to landscape-scale invasion dynamics and management: a case study of lionfish metapopulation". In: *Philosofical Transactions of the Royal Society B* 374 (Mar. 2019) (cit. on p. 3).

[VS18] Aram Vajdi and Caterina Scoglio. "Identification of Missing Links Using Susceptible-Infected-Susceptible Spreading Traces". In: *IEEE Transactions on Network Science and Engineering* 6 (4 2018), pp. 917–927 (cit. on p. 7).

[VW02] P. Van den Driessche and J. Watmough. "Reproduction numbers and sub-threshold endemic equilibria for compartmental models of disease transmission". In: *Mathematical Biosciences* (2002). DOI: https://doi.org/10.1016/S0025-5564(02)00108-6 (cit. on pp. 4, 5).

[Wan+11] W.-X. Wang et al. "Time-series based prediction of complex oscillator networks via compressive sensing". In: *Europhys. Lett.* 94 (2011) (cit. on p. 6).

[Wax88] B. M. Waxman. "Routing of multipoint connections". In: *IEEE J. Select. Areas Commun.* 6 (9 1988), pp. 1617–1622 (cit. on p. 16).

[WL19] J. A. Ward and López-García. "Exact analysis of summary statistics for continuous-time discrete-state Markov processes on networks using graph-automosphism lumping". In: *Applied Network Science* 4 (1 2019) (cit. on pp. 7, 8).

[WZ05] Wendi Wang and Xiao-Qiang Zhao. "An Age-Structured Epidemic Model in a Patchy Environment". In: *SIAM Journal on Applied Mathematics* 65 (5 2005), pp. 1597–1614 (cit. on pp. 4, 5).

[YCN21] Jean-Gabriel Young, George T Cantwell, and M E J Newman. "Bayesian inference of network structure from unreliable data". In: *Journal of Complex Networks* 8.6 (Mar. 2021). cnaa046. ISSN: 2051-1329. DOI: 10.1093/comnet/cnaa046. eprint: https://academic.oup.com/comnet/article-pdf/8/6/cnaa046/36509950/cnaa046.pdf. URL: https://doi.org/10.1093/comnet/cnaa046 (cit. on p. 6).

[YGJ08] Hyejin Youn, Michael T. Gastner, and Hawoong Jeong. "Price of Anarchy in Transportation Networks: Efficiency and Optimality Control". In: *Physical Review Letters* 101 (Sept. 2008) (cit. on p. 3).

[YP10] D. Yu and U. Parlitz. "Inferring local dynamics and connectivity of spatially extended systems with long-range links base on steady-state stabilization". In: *Physical Review E.* 82 (Aug. 2010) (cit. on p. 5).

[YTC02] M. Yeung, J. Tegnér, and J. Collins. "Reverse engineering gene networks using singular value decomposition and robust regression". In: *Proceedings of the National Academy of Sciences USA* 99 (9 2002), pp. 6163–6168 (cit. on pp. 5, 6).